FINAL REPORT

Investigating the Effects of Chronic Turbidity Exposure to Priority Florida Coral Species

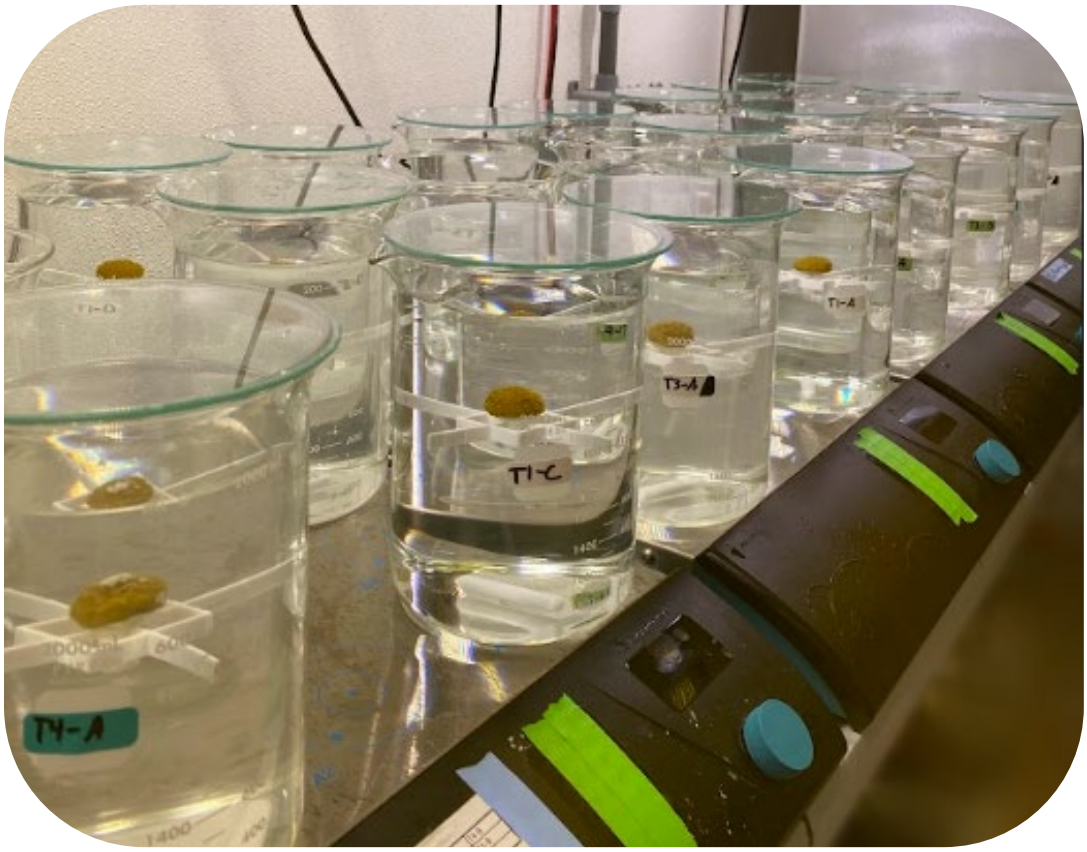

Florida Department of Environmental Protection
Coral Protection and Restoration Program

Investigating the Effects of Chronic Turbidity Exposure on Priority Florida Coral Species

Final Report

Prepared By:

Courtney M. Saldaña[1], Carl V. Miller[2], Zachary J. Moffitt[1], Ray M. Radick[1], Arielle Pollock[1], Janet E. Saunders[1], E. Murphy McDonald[1], Ronald T. Kothera[1], Lisa A. May[1], and Cheryl M. Woodley[2]

[1]Consolidated Safety Services, Inc. contractor for NOAA, NOS, National Centers for Coastal Ocean Science, Hollings Marine Laboratory, 331 Ft. Johnson Rd., Charleston, SC 29412, United States of America
[2]NOAA, NOS, National Centers for Coastal Ocean Science, Hollings Marine Laboratory, 331 Ft. Johnson Rd., Charleston, SC 29412, United States of America

June 15, 2024

Completed in Fulfillment of PO C1FE5B (MOA-2021-018/12072 Amendment 001) for

Florida Department of Environmental Protection
Coral Protection and Restoration Program
8000 N Ocean Dr.
Dania Beach, FL 33004

This report should be cited as follows:

Saldaña CM, Miller, CV, Moffitt ZJ, Radick RM, Pollock A, Saunders JE, McDonald EM, Kothera RT, May LA, and Woodley CM. 2024. Investigating the Effects of Chronic Turbidity Exposure on Priority Florida Coral Species. Award no. C1FE5B. Florida DEP. Miami, FL, 70p.

This report was prepared for the Florida Department of Environmental Protection (DEP) by the National Oceanic and Atmospheric Administration (NOAA), National Ocean Service (NOS), National Centers for Coastal Ocean Science (NCCOS). Funding was provided by FL DEP award no. C1FE5B through a Memorandum of Agreement between the FL DEP, Coral Protection and Restoration Program and NOAA, NOS, NCCOS. The views, statements, findings, conclusions, and recommendations expressed herein are those of the author(s) and do not necessarily reflect the views of the State of Florida or any of its sub-agencies.

Acknowledgements
We extend our gratitude to the Florida Department of Environmental Protection's Coral Protection and Restoration Program (DEP, CRP) for supporting this project and particular thanks to the project managers, Patrick Connelly, Kristi Kerrigan and Kylie Morgan for review feedback and discussions to optimize the management relevance of this work. The authors would like to express a special thanks to Mark Ladd and Xaymara Serrano, of the National Marine Fisheries Service for collecting the sediment samples used in this project. We thank Jennifer Ness, National Institute of Standards and Technology, Charleston, SC for assistance with the particle size analysis of the turbidity treatment solutions and Samantha Helmericks for her help with histology. We also thank Jocelyn Karazsia, Xaymara Serrano, Mark Ladd and Keisha Bahr for helpful discussions in experimental designs. The authors acknowledge and are appreciative of the use of facilities in the Hollings Marine Laboratory, supported by NOAA, NOS, NCCOS and the histology facility at South Carolina Department of Natural Resources.

Management Summary (300 words or less)
Florida DEP, Coral Protection and Restoration (CPR) Project C1FE5B (MOA-20210018/12072 amendment 1) was developed in conjunction with resource managers to begin filling priority knowledge gaps related to the effects of turbidity on the Endangered Species Act (ESA)-listed coral, *Orbicella faveolata*, in relation to anthropogenic activities (e.g., coastal construction, dredging) that can create turbid conditions in exceedance of the Florida water quality criterion (WQC) of 29 NTU above natural background. Because of *O. faveolata's* (1) ESA status, (2) Critical Habitat designation for recovery of the species, (3) ecological importance as a major reef-building species, and (4) its population density in areas expected to experience prolonged periods of anthropogenic turbidity from planned dredging operations, understanding the tolerance for turbidity is imperative for effectively protecting Florida's Coral Reef. Our objectives were (1) to identify biological benchmarks for turbidity that are protective for shallow-water corals and (2) to design experiments with assessment endpoints that are able to detect and measure sub-lethal impacts on coral health while also useful to resource managers responsible for minimizing impacts from anthropogenic turbidity affecting reefs. We investigated two aspects of chronic turbidity exposure: dosage effects (turbidity range 0-29 NTU) and effects of combined turbidity (29 NTU) and elevated temperature (30 °C) over a 90-day period. We observed that *O. faveolata's* ability to heal wounds (bioindicator of health and fitness) was significantly decreased after prolonged exposure to 20 and 29 NTU at 28 °C, revealing an important impact on coral physiology in response to turbidity lower than the existing WQC. An increase of 2 °C (to 30 °C) combined with 29 NTU reduced wound healing rates, growth rates and total lipid concentrations. Turbidity (29 NTU) alone reduced triglyceride concentrations (energy reserves) and wound healing. Knowing the potential consequences of compounding effects on vital physiological processes with a non-bleaching temperature increase, provides managers key insights for how *O. faveolata* may be impacted during summer temperatures and potentially more severely with predicted bleaching conditions. This provides an opportunity for managing impacts during turbidity-producing operations, that can occur even within the existing WQC.

Executive Summary

Marine resource managers are constantly faced with an escalating number and magnitude of threats in coastal areas, from growing tourism, coastal construction, urbanization and new industries. These threats bring new challenges to the marine environment, especially for managing water quality. Florida's Coral Reef (FCR) is threatened by numerous water quality issues (e.g., eutrophication, pollutants, acidification, sedimentation, turbidity, etc.) driven or exacerbated by a variety of anthropogenic activities. Coastal construction and dredging are two significant sources of anthropogenic turbidity (i.e., decreases in water clarity from sediment suspension) that have been reported to cause habitat destruction and negative impacts on marine species (Dodge and Vaisnys 1977; Miner and Stein 1996; Anthony and Fabricius 2000; Jones et al. 2016 Stauber et al. 2016; Wahab et al. 2017; Tuttle and Donahue 2022). Two large multi-year dredging operations are planned for Southeast Florida that are expected to generate sustained turbid conditions in these areas. Threatened coral species, including *Orbicella faveolata* populations, also inhabit these potential danger zones. Dredging operations are monitored to control turbidity levels using Florida's turbidity water quality criterion (WQC) (29 nephelometric turbidity units (NTU) above natural background) (US Environmental Protection Agency 1988). However, it is unknown whether the existing WQC protects coral and other reef organisms from impacts expected from these dredging operations.

The impetus for this project (C1FE5B) was the need by FL Department of Environment Protection (DEP) for turbidity biological benchmarks for shallow-water coral. This project investigated two aspects of chronic turbidity exposure: 1) dosage effects (turbidity range 0-29 NTU) and 2) effects of combined turbidity and elevated temperature (30 °C) over a 90-day period. *O. faveolata* was used in these studies (1) because of its threatened listing under the ESA, (2) being ecologically critical as reef builders, (3) as vulnerable populations inhabiting potentially hazardous dredging zones, and (4) expected to experience chronic turbidity over prolonged periods. Native sediment from the entrance channel area of Port Everglades (FL) was used to minimize variation in effects which is known to occur with different sediment types (Tuttle and Donahue 2022).

We quickly learned that turbidity studies, thought to be easy laboratory experiments, were very challenging. This led to several months of turbidity trials to optimize experimental conditions for rigorous control of water quality parameters. This report details the workflow required to achieve sediment grain sizes (avg. 19.9-30.6 μm) that are suitable for generating targeted turbidity levels, and which mimic water column grain sizes reported during dredging activities (Enochs et al 2019; Jones et al 2016; Wang and Beck 2017). This involved drying and milling the native sediment in a cryomill, specific mixing and vessel filling protocols. Though complex systems to generate turbidity treatments are described in the literature (Jones et al. 2020), our objective was for a simple design, easily repeated by others with materials easily sourced. This is reflected in using glass beakers with stir bars, custom-built water baths and commercially available

lighting and controllers. The time spent on this R&D resulted in highly stable turbidity and water quality parameters (pH, salinity, temperature) throughout the project.

This study evaluated the effect(s) of chronic turbidity on the condition of *O. faveolata* from two perspectives, (1) different turbidity levels (dosage) and (2) a single turbidity level combined with an elevated temperature, that is below the bleaching threshold for this species. Both experiments used a combination of non-invasive and invasive assessment endpoints. Non-invasive endpoints were used to measure changes through time and cumulative effects at 90 days. For growth, the data provided a growth curve and growth rate over time, as well as the total growth for each treatment after 90 days. The photosynthetic performance of the algal symbionts also was assessed with weekly measurements of photosynthetic efficiency (Fv/Fm) over the course of the experiment. Although invasive, the ability of the fragments to recover from the trauma of an intentional laceration after being exposed to turbidity or turbidity with elevated temperature for 10 weeks was also profiled over the last two weeks of both experiments. Lastly, terminal endpoints also were assessed, only capturing an ending snapshot of the cumulative impacts. These were measures of energy stores (total soluble proteins, total lipids and triglycerides, a subclass of energy-related lipids, measured only in the elevated temperature/turbidity experiment). Algal symbiont densities that can influence photosynthetic performance and nutrient supply for the coral host were measured from histological sections.

The first experiment asked: *Does turbidity level (dose) at or below the current water quality criterion under fixed conditions of duration and normal temperature, adversely affect O. faveolata?*

The data show that growth is not affected by turbidity levels of 0-29 NTU after 90 days at an optimal temperature (28 °C). Each of the turbidity levels seems to invoke processes that allow the algal symbionts to acclimate to the new conditions and compensate for the disturbance (i.e., turbidity) by increasing photosynthetic efficiency over time. This increase maybe considered an indication that a new energy-demand has been placed on the holobiont and photoacclimation is one mechanism algae use to off-set the energy expenditures from this response. Together these data indicate that the test organisms can respond and acclimate to all of the turbidity levels with no adverse effect after 90 days. This experiment cannot predict how long these corals can sustain this functional level, i.e., if the duration doubled would these fragments still be able to maintain growth performance and a higher level of photosynthetic efficiency, is unknown. There is a hint in the biochemical data that suggests the energy reserves (protein and lipid) are potentially being depleted at a rate greater than they are being replenished, but not to the extent that physiological damage is indicated. One of the assessment endpoints that may be of concern is the muting of the wound healing rate over the 90 days. Although ultimately most of the fragments healed, there were obvious differences in the time required for the wounds to heal in all of the turbidity treatments (10 NTU = 2.6-day delay, 20 NTU = 5-day delay and 29 NTU = 4.4-day delay). These delays represent a point of vulnerability for the coral as the prolonged exposure of open wounds provides additional time for opportunistic invasions (e.g., algae, microbes, pollutants) that otherwise would be protected with an intact tissue barrier.

The second experiment asked: *Does a two degree increase in temperature (above normal culture conditions) coupled with exposure to a fixed turbidity level of 29 NTU and duration, adversely affect O. faveolata?*

The data show that with elevated temperature and turbidity the trend in photosynthetic efficiency over the 90 days is depressed compared to 0 and 29 NTU conditions at 28°C. This indicates that the process of photoacclimation is being challenged when compared to the results in the first experiment that showed a robust ability for photoacclimation. By the end of 90 days, all treatments seemed to be converging to the same maximum quantum yield, albeit lower than the initial Fv/Fm. Although not significant (likely due to the variation between replicates), there is a trend showing a decrease in symbiotic algae density in samples exposed to turbidity (regardless of temperature) which supports the maximum quantum yield data of a depressed response to photoacclimation. Total growth and growth rate were both reduced with turbidity; increased temperature further retarded growth. Wound healing rate was reduced with turbidity exposure, though elevated temperature seemed to provide a degree of compensation by increasing growth rates in the 0 and 29 NTU treated fragments, compared to the 28°C treatments. Further, the amount of tissue regenerated under the high temperature/high turbidity treatment (30°C, 29 NTU) was significantly less than the low temperature/no turbidity treatment (28°C, 0 NTU) by the end of the 14-day healing period. Each of these processes require energy to fuel the responses to new disturbances that challenge the plasticity boundaries of physiological responses (e.g., turbidity combined with small temperature increases). The ability to maintain energy reserves is one of the factors that determines the organism's phenotypic plasticity to accommodate an altered state and successfully respond to environmental stressors through acclimation or acclimatization. If the phenotypic (i.e., physiologic) plasticity of the organism is overwhelmed, then impacts to fitness occur. Our data show that under the conditions and duration of this experiment *O. faveolata* fragments were able to maintain their soluble protein and total lipid pools. Interestingly, the elevated temperature without turbidity significantly increased the total lipid content. This positive response was ameliorated when both elevated temperature and turbidity were present, as the nubbins with combined stressors could only maintain lipid levels comparable to the 28 °C controls. However, when just the triglyceride subclass of lipid was measured, corals in either turbidity treatment showed significantly less triglyceride concentrations. Further, though not statistically significant, the no turbidity and elevated temperature also showed a trend toward a lower concentration. Together these data indicate there is a physiological and energetic cost to the *O. faveolata* nubbins with turbidity exposure that can be increased with elevated temperature. These corals are showing multiple signs of stress and challenges to key processes such as growth and wound healing as well as declines in photosynthetic efficiency and triglyceride stores that function to support cellular metabolism. Our data seem to indicate that we are at or near a threshold tipping point. Our assessment endpoints do not support the conclusion of no impact or that acclimation or acclimatization processes are robust against turbidity levels at the water quality criterion when a small increase in temperature is added to this initial stressor. We are unable to predict whether with additional time under these conditions, the coral will return to their prior physiological state, acclimate to a new state, or continued exposure will prevent recovery once the stressors are removed.

Table of Contents

1. BACKGROUND

Water quality issues (e.g., turbidity, sedimentation, eutrophication, pollutants, etc.) are threats to Florida's Coral Reef (FCR). The Coral Protection and Restoration Program (CPR) in the Florida Department of Environmental Protection (DEP) recognizes the urgent need for water quality protection and to identify biological benchmarks as a vital step to managing water quality stressors. However, biological benchmarks have not been clearly established for many of the water quality parameters with respect to protection of near shore shallow coral reef organisms. The protection offered by the existing turbidity water quality criterion is of particular interest to the DEP, CPR Program at this time because of major coastal construction projects pending in the state that could threaten nearby coral reef ecosystems, including several species (*Orbicella faveolata, Acropora cervicornis*) listed as threatened under the Endangered Species Act of 1973, as amended (Federal Register 2006, 2014).

Turbidity is a key water quality parameter that represents the optical clarity (light absorbed or scattered) of the water column and which is affected by suspended sediment, and dissolved and particulate organic matter (Kitchener et al. 2017; Zweifler et al. 2021). Turbidity can occur from natural processes (e.g., runoff from rain or storm events, river outflows, resuspension, geological disturbances) and from anthropogenic activities (e.g., sewage outfalls, coastal construction, agricultural practices, eutrophication, industrial activities, i.e., mining, logging, dredging) (reviewed in Zweifler et al. 2021). The degree to which coral reefs are impacted by turbidity depends on the frequency, magnitude, duration of turbid conditions, composition of the sediment and the susceptibility of affected species (Jones et al. 2016; Tuttle and Donahue 2022). However, quantitative data to determine impact thresholds are lacking (Macdonald et al. 2013; Zweifler et al. 2021; Santana et al. 2023).

The Florida standard operating procedures adopted nephelometry as the methodology for measuring turbidity (DEP-SOP-001/01, FT1600). The turbidity water quality criterion for Florida states that levels are not to exceed 29 nephelometric turbidity units (NTU) above natural background (Florida Administrative Code 2016; US Environmental Protection Agency 1988) with natural background turbidity averaging approximately 1-2 NTU in near-shore waters (Whitall et al. 2019). The data used in establishing the current turbidity criterion did not include data for potential impacts to coral or other coral reef organisms, and little data is available to warrant re-evaluation of the criterion. Florida is currently in the planning phase for two large multi-year dredge projects: Port Everglades and Port of Miami (combined direct removal of coral reef is approximately 50 acres or 202,000 m^2), and also smaller maintenance dredge operations in both ports with both operations located amidst coral reef ecosystems. Therefore, the State of Florida is seeking data on turbidity impacts to naturally occurring corals and other key reef organisms likely affected in these disturbance zones. To fill this knowledge gap, acute and chronic turbidity exposure studies to identify biological benchmarks that are protective of Florida's Coral Reef are critically needed to inform decision-makers charged with managing these and similar projects that generate turbid conditions over extended periods of time.

Anthropogenically driven turbid conditions in proximity to natural reefs can have a number of harmful effects on coral and reef ecosystems that are not overt mortality, but

are sublethal, compromising physiological processes and undermining fitness (Sheridan et al. 2014; Ashley et al. 2024). Corals do possess several defense mechanisms used in response to turbidity stress, which include sediment shedding mechanisms (increased mucus production, ciliary beating, polyp inflation) (Stafford-Smith 1993; Sheridan et al. 2014), increased photosynthetic efficiency under low-light conditions (Hennige et al. 2008; Larsen et al. 2017), and shifts to heterotrophic feeding (Anthony and Fabricius 2000). However, when stress responses and acclimation processes are overwhelmed, corals can exhibit depleted energy reserves, abrased tissue, photosynthetic dysfunction, induction of immune responses, increased disease susceptibility, impaired nutritional status, impaired reproductive effort and other debilitating effects that reduce fitness and growth (reviewed in Erftemeijer, et al. 2012; Jones et al. 2016; Zweifler et al. 2021).

Orbicella faveolata, the mountainous star coral, was a priority species for this project due to its proximity to major coastal construction projects in Southeast Florida, and having knowledge gaps with respect to adverse effects that anthropogenic turbidity has on the health and fitness of this species. These corals are long-lived and critical as framework developers of reefs and critical to the surrounding ecology of western Atlantic and Caribbean reefs (Bruckner 2012). The species range from Palm Beach County in Southeast Florida to the Dry Tortugas in Florida and Puerto Rico, the USVI and Navassa Island and into the Flower Garden Banks National Marine Sanctuary in the Gulf of Mexico where they commonly occupy depth ranges of 15-30 m, but can range from 5-50 m (NMFS 2024). Over the last 30 years, this species has experienced a precipitous population decline from disease, bleaching, predation and pollution (Bruckner 2012; NMFS 2024). In 2009, the Center for Biological Diversity petitioned the National Marine Fisheries Service (NMFS) to list this species along with 82 others as threatened or endangered. Based on the findings, NMFS listed *O. faveolata* (and 19 other species) as threatened under the Endangered Species Act (ESA) of 1973, as amended (Federal Register 2014). In 2023, as a result of its ESA status, the areas occupied by *O. faveolata,* with physical and biological features required for its conservation, were designated as critical habitat (Federal Register 2023). Thus, due to its ESA status and the critical roles *O. faveolata* plays in the structure and function of reefs, it is imperative that those charged with overseeing the recovery of this species have sufficient data and information on which to base management decisions.

This project was developed in conjunction with resource managers to begin filling priority knowledge gaps by investigating effects of chronic turbidity exposures (90 days). We used both a dose-response challenge experiment (turbidity range 0-29 NTU) and a dual stressor challenge experiment (combined effect of turbidity (29 NTU) and elevated temperature (30 °C)) on *O. faveolata* fragments. Naturally occurring sediment was collected from Port Everglades, FL and used in this project to simulate natural sediment characteristics in a controlled laboratory setting. Physiological, histological and biochemical indicators for growth, tissue regeneration, photosynthetic efficiency, algal symbiont density and energy reserves, essential to fitness and survival, were used in evaluating potential impacts to this ESA-listed coral.

2. MATERIALS AND METHODS

2.1. Coral source and culture conditions

The *Orbicella faveolata* source colony is a long-term (>20 years) holding of the NOAA National Centers for Coastal Ocean Science Charleston Laboratory coral culture facility. Here, several *O. faveolata* colonies are held under a Florida Keys National Marine Sanctuary permit (#FKNMS-2016-021) and a South Carolina Department of Natural Resources non-indigenous species permit (#NI24-348). Culture systems consist of a (750 L) recirculating glass and Teflon aquaria filled with artificial seawater (ASW, B-Ionic Seawater System, ESV Aquarium Products, Hicksville, NY, 36 ppt) and maintained at 28 ± 1 °C with a 300 W submersible glass heater (Jager TruTemp, Eheim, Deizisau, GER) and a ¼-hp cyclone drop-in chiller (Aqua Logic Inc., NC). The recirculating aquaria systems include a sump with a custom glass protein skimmer and refugium that provides biological filtration while five LED light fixtures (Radion XR30 G5 Pro, Ecotech Marine, Lehigh County, PA) provide an irradiance (photosynthetically active radiation) range of 160-170 µmol photons m^{-2} s^{-1} on a 12.5 h:11.5 h light:dark cycle with a customized spectrum; color channels include UV 50 %, violet 50 %, royal blue 50 %, blue 50 %, red 100 %, green 25 %, cool and warm white, each 100 %. Alkalinity, calcium and trace mineral levels as well as total alkalinity (143-161 mg/L $CaCO_3$) and pH (8.1-8.3) were regulated with custom glass calcium reactors (Greatglas, Inc., Wilmington, DE) via a manual drip system. In culture, corals were fed three times per week a maintenance diet of New Life Spectrum (New Life International Inc., FL, USA) Reef Cell Large (400-600 µm), Grow Cell Medium (300-400 µm), Reef Cell Small (10-80 µm), Reef-Roids (PolypLab, QC, Canada), as well as the following frozen foods: cyclops, copepods, red plankton (*Calnus* sp.), mysis shrimp, and rotifers (Gamma Slice, Tropical Marine Centre™ Hertfordshire, UK).

A Gryphon AquaSaw with diamond band saw blade was used to rough-cut a sufficient number of 1.5 cm diameter nubbins for this project from the source colony that then were shape-finished using a Dremel tool with diamond cutting wheel. Nubbins were attached to custom Teflon mounting pegs with cyanoacrylate gel (Seachem Reef Glue™) as detailed in May et al. (2020) and allowed to completely heal (minimum of 16 weeks) in the main culture system prior to testing.

2.2. Sediment source and cryomilling

Sediment for the turbidity experiments was provided by Florida DEP. Surface sediment from a depth of approximately 35 m was collected in July 2023 from approximately 800 m outside the Port Everglades, FL entrance channel (1 site north and 1 site south of the channel) in proximity to coral reef habitat by divers from the National Marine Fisheries Service. Divers used a scoop to collect sediment which was placed into Teflon bags (5 mil, PFA, Welch Fluorocarbon, Dover, NH) and held at 4 °C. Prior to shipping, the sediment was pooled, mixed thoroughly to homogenize and bagged into three aliquots to support three separate DEP projects. One aliquot was shipped to the NOAA NCCOS laboratory in Charleston, SC. Upon arrival,

sediment was apportioned into 500 mL glass jars and fully dried at 105 °C from 16 to 72 h. After cooling, the portions were pooled and mixed to homogenize the sediment. Sediment was cryomilled to a fine consistency using three separate 3 min milling cycles under liquid nitrogen using a SPEX Certi-Prep cryomill (Metuchen, NJ) set at 10 cycles per second.

2.3. Stock turbidity preparation

Artificial seawater (ASW) (ESV B-Ionic, 36 ppt) for all treatment solutions was mixed in a 265 L polypropylene reservoir using Type 1 water at 27 °C – 28 °C for 24 h. Treatment solutions were generated by pumping ASW into large (55 L) clean glass carboys (Greatglas, Inc., Wilmington, DE) containing a Teflon PTFE stir bar (70 x 20 mm, oval; Cole-Parmer Cat. # UX-04768-85) for mixing on 11" x 11" stir plates (Corning® Top PC-611 Stirrer). Treatment solutions were created by adding the cryomilled, dried sediment to the 55 L carboy of ASW as follows: 6 g for 10 NTU, 11 g for 20 NTU and 16 g for 29 NTU. These proportions gave an exceedance of 3-5 NTU above the intended experimental NTU level to allow for final adjustments to the target NTU. Vessels were covered with polypropylene lids to prevent evaporation and contamination, and mixed (stir level 9-10) for 24 h (27 °C – 28 °C in a temperature-controlled room). After mixing, turbidity was measured using a Hach model 2100Q turbidimeter calibrated with Hach StablCal® formazin standards prior to use and in accordance with Florida DEP SOP FT1600 Field Measurement of Turbidity (Florida Department of Environmental Protection 2023).

If turbidity fell below the targeted NTU treatment, additional sediment was added (~1 g at a time) and the solution was mixed for at least one hour before re-measuring turbidity. After turbidity was verified, mixing was halted for approximately 1 min to allow heavy sediments and aggregated particulates to settle to the bottom of the carboy which were then siphoned out using Teflon tubing, removing approximately 4-6 L. This volume was replaced with ASW to adjust treatments to the final NTU targets. Mixing was resumed for 15 min and turbidity was checked to verify the experimental targeted NTU had been achieved. If turbidity was above the experimental target, ASW was added (while mixing) to dilute the mixture to the targeted NTU according to **Equation 1**:

Equation 1:
V = 55 L – [(T/M) x 55 L],
where V = dilution volume (in liters),
T = turbidity target (NTU) and
M = measured turbidity (NTU)

2.4. 90-day turbidity dose-response experiment

2.4.1. Experimental design

The chronic 90-day experiment was carried out with four treatments (ASW control and processed sediment at 10, 20, 29 ± 2 NTU) at 28 °C in glass beakers (all

raw data found in Appx. 6.1.A & 6.2.B; detailed protocol Appx. 6.4.D1). Acclimation vessels (2 L test volume) were identical to treatment vessels, except they were filled with ASW rather than treatment solution. Vessels held Teflon-coated stir bars and egg crate louver coral support stand positioned approximately 6.5 cm below the surface and were filled with treatment solutions from appropriate stocks in a temperature-controlled challenge room (27 °C -28 °C) (**Figure 1**). Vessels were placed randomly onto magnetic stir plates (JEIO TECH, Multi-Channel Stirrer, Model: MS-53M) that were set at 300 rpm to keep sediment suspended. Irradiance (photosynthetically active radiation (PAR)) was provided with two Ecotech Marine Radion XR30 G5 PRO lights. The dose-response experiment had a PAR of 154 ±12 µmol photons m^{-2} s^{-1} and the dual stressor experiment had a PAR of 156 ±10 µmol photons m^{-2} s^{-1} with a 12.5 h light:11.5 dark light cycle. These conditions emulated those in the aquaculture system.

A total of 30 *Orbicella faveolata* coral nubbins (24 experimental, 6 time-0) were fed just prior to acclimation. Nubbins then were transferred using Teflon-coated tongs to acclimation vessels (2 L glass beakers) with the Teflon mounting pegs attached to coral placed into the custom egg crate louver (acrylic) stands situated at the 1200 mL line of treatment vessels (6.5 cm from surface and 9.5 cm from the bottom, nubbins approximately 1 cm in height). Vessels were placed in randomly assigned positions on the magnetic stir plates. Acclimation proceeded for four days to test system conditions prior to starting the experiment. During the four-day acclimation period, temperature, salinity, and pH measurements were obtained for a single random replicate for each treatment.

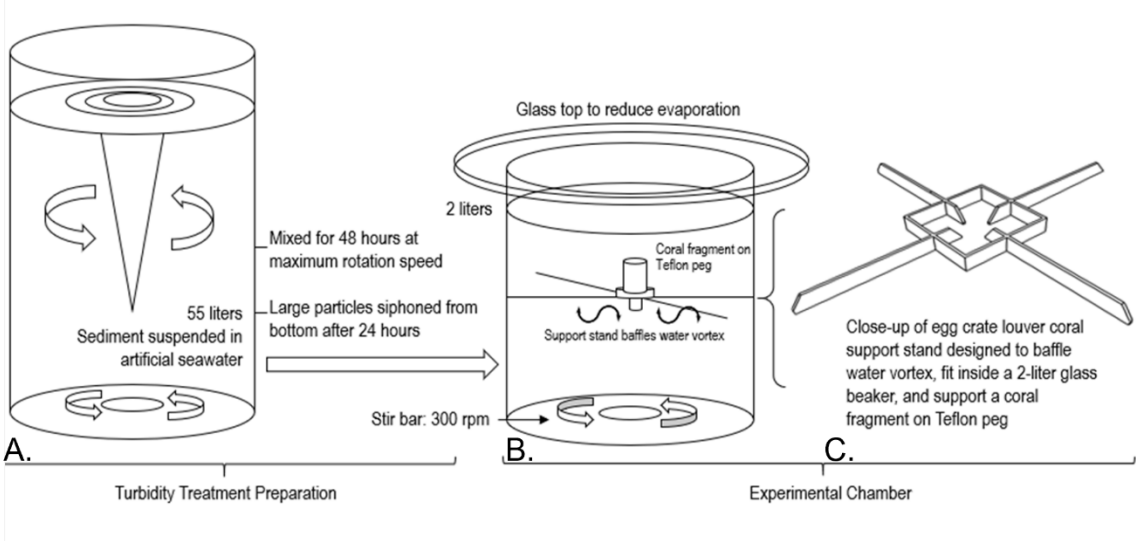

Figure 1. Illustration of the final design for turbidity stock preparations (A) and exposure chambers (B) with detailed view on how nubbins were supported in beakers (C).

At the start of the experiment, a single coral nubbin was transferred to each clean treatment vessel (cleaning methods modified from US Environmental Protection Agency 1980; see Appx. 6.4.D3), which was filled with an assigned treatment solution of 0, 10, 20, or 29 NTU. Treatment changes were performed using a silicon

hose and Mag-Drive 2 pumps (Danner Manufacturing, Inc. Islandia, NY) attached to the bottom spigot of each glass carboy, with flow controlled by a ½" polypropylene ball valve on the end of each hose while corals were being imaged and weighed. Treatments were pumped into clean treatment beakers to a final volume of 2 L. After each test fragment was measured, new (fresh) treatments and beakers with their respective coral fragment were placed on multi-position magnetic stir plates in the same randomized positions as the acclimation vessels. Corals were transferred from acclimation vessels to the treatment vessels using clean Teflon-coated tongs and mixing (300 rpm) was initiated. Experiments proceeded with once-daily resuspension of any sediment that settled using a 3 mL disposable transfer pipette to gently flush sediment from the coral and/or coral stand. Turbidity was measured just before and just after sediment resuspension to give daily minimum and maximum turbidity values. The calibration and verification requirements in FT1000 and FT1600 (Florida Department of Environmental Protection 2023) were followed and included in the study design (Appx. 6.4.D1).

At time-0, just prior to experiment initiation recurring endpoint measurements were made. Weekly measurements for: 1) maximum quantum yield (Fv/Fm) based on symbiont chlorophyll *a* fluorescence was obtained from dark-adapted coral ~30-45 min prior to lights coming on (details in section 2.7.1 and Appx. 6.4.D5 for protocol); nubbin buoyant weight (detailed in section 2.8.1 and Appx. 6.4.D7 for protocol); and nubbin bright field and fluorescence photomacrographs for monitoring color or morphological change (see Appx. 6.4.D8). For imaging, nubbins were placed in a crystallizing dish filled with fresh ASW and imaged with MVX10 research macro zoom microscope equipped with a 0.63x objective (Olympus, Melville, NY) (filter #U-MWB2: excitation: 460-4190 nm; emission (barrier filter): 529IF*2 nm; dichromatic mirror: DM500 nm; Chroma Technology Corp, Bellows Falls, VT) and a DP71 digital camera (Olympus, Center Valley, PA). Exposures were 8 ms for bright field and 500 ms under a wide blue filter for fluorescence. Daily photomacrographs were taken after wounding coral two weeks prior to experiment termination, as a tissue regeneration assay was initiated (detailed in section 2.8.2 and Appx. 6.4.D8 for protocol). Throughout the experiment, coral specimens were fed for at least 2 h prior to a twice-weekly water and beaker change (Tuesdays and Fridays) with 2 mL of an equal mix of Reef-Roids (Polyp Lab, Montreal, Canada), Reef Cell Small (10-80 µm) food (New Life Spectrum, Homestead, FL), and Grow Cell Medium (300-400 µm) (New Life Spectrum) in ASW (for additional information, please see experimental protocol in Appx. 6.4.D1).

2.4.2. Water quality

Salinity, temperature, and pH were measured in treatment vessels prior to treatment renewal ("Spent" solutions) on Tuesdays and Fridays using a Thermo Scientific ORION Star A329 pH/ISE/conductivity/ROD/DO meter S/N-G13613 equipped with two probes: pH probe, ORION 8107UWMMD Ross ultra pH/ATC triode and conductivity probe, ORION 013010MD conductivity cell. Salinity and pH were measured from the stock solution ("Fresh") on treatment renewal days and turbidity was measured before and after treatment renewals. Before treatment change, 15 mL spent treatment solution was collected from each treatment vessel in a 20 mL

sample cell (Hach 2100 portable turbidimeter sample cells, # 2434702) that was inverted gently about three times before placing in the turbidimeter. Following treatment renewal, 15 mL of fresh treatment media was collected and measured similarly. On the other days (Mondays, Wednesdays, Thursdays, Saturdays, and Sundays), turbidity was measured before ("Pre") and after ("Po") resuspending sediments accumulated on coral and/or stands and beakers by gentle flushing with a 3 mL disposable transfer pipette. Temperature was measured on non-treatment renewal days using a digital thermometer (ThermoPen, ThermoWorks, American Fork, UT). Both temperature probe and thermometer were verified with a NIST Traceable thermometer (Manufacturer: Control Company, distributed by VWR International LLC, Model:89369-138, S/N: 230028217) according to the calibration and verification requirements in Florida DEP SOP FT1000 and FT1400 (Florida Department of Environmental Protection 2023) (**Table 1**).

Table 1. Calibration frequency and verification of water quality instruments. Calibrations and verifications were performed based on Florida SOPs FT1000, FT1400, FT1100, FT1200, and FT1600 (Florida Department of Environmental Protection 2023). Instruments also were calibrated if battery replacement occurred or a verification measurement did not meet the acceptance criteria for each respective Florida SOP. *Probe used in parallel with a Thermo Scientific ORION Star A329 pH/ISE/conductivity/ROD/DO hand held meter.

Parameter	Equipment	Calibration Frequency	Verification Frequency	Measurement Frequency
pH	ORION 8107UWMMD Ross Ultra pH/ATC Triode*	Immediately prior to experiment initiation and weekly there after	Immediately after calibration and biweekly prior to use	Biweekly on both fresh and spent treatments
Salinity	ORION 013010MD Conductivity Cell*	Immediately prior to experiment initiation and weekly there after	Immediately after calibration and biweekly prior to use	Biweekly on both fresh and spent treatments
Temperature	ORION 013010MD Conductivity Cell*	N/A	Immediately prior to experiment initiation and quarterly there after	Biweekly on spent treatments
Temperature	Thermoworks Thermapen Mk4 Digital Thermometer	N/A	Immediately prior to experiment initiation and quarterly there after	Daily
Turbidity	HACH 2100Q Portable Turbidimeter (CAT#-2100Q01)	Immediately prior to experiment initiation and quarterly there after	Immediately after calibration and daily prior to use	Twice daily

2.5. 90-day dual stressor experiment

2.5.1. Experimental design

The turbidity level used in the dual stressor experiment (29 NTU) was based on sub-lethal results from the dose-response experiment. Exposures with a combination of 29 NTU and an elevated temperature of 30 °C were designed to investigate the chronic effects of these stressors over 90 days (see Appx. 6.4.D2 for detailed protocol). A total of four treatments were tested, an ASW control and a turbidity treatment (29 ± 2 NTU), each at 28 °C and 30 °C, with six replicates in each treatment (n=24). The experimental set up was similar to the dose-response experiment as was the endpoint data collection (detailed in section 2.4.1). Test temperatures were achieved using two custom built glass water baths, each placed over two multi-position stir plates (JEIO TECH, Multi-Channel Stirrer, Model: MS-53M). Each water bath was plumbed to a sump equipped with a magnetic drive model 5 return pump (Danner Manufacturing, Inc., Islandia, NY), two 300 W titanium heaters, and a temperature probe connected to an Apex A3 controller. The Apex was set to turn on one heater in each sump when the temperature probe readings dropped to 27.8 ˚C and 29.8 ˚C, respectively, and turn off when readings rose to 28.0 ˚C and 30.0 ˚C. The second heater in each sump was set to turn on when the temperature probe readings dropped to 27.5 ˚C and 29.5 ˚C, respectively, and turn off when readings rose to 28.0 ˚C and 30.0 ˚C. The second heater was a failsafe in the event the first heater malfunctioned (for additional information, please see Appx. 6.4.D2 for protocol details).

2.5.2. Coral acclimation to test conditions

Approximately four weeks prior to initiating the experiment, the experimental, 30 °C test group was ramped from 28 °C to 30 °C. *Orbicella faveolata* nubbins were placed in two 75.7 L (20-gallon) tanks each at 28 °C with an irradiance of ~150 μmol/(cm^2·s) to mirror aquaculture conditions. A total of 32 coral (24 experimental, 8 time-0) nubbins were randomly assigned to treatments, with 16 nubbins in each tank for temperature acclimation. The first tank was maintained at 28 °C for the duration of temperature acclimation (1/12/2024-2/8/2024). Nubbins from this tank were used for treatments exposed to 28 °C (0 NTU and 29 NTU treatments). Temperature for the second tank was increased over a five-day period (1/16/2024-1/20/2024) to 29 °C with daily increments of 0.2 °C, and then raised to 30 °C with daily increments of 0.1 °C, over a ten-day period (1/21/2024-1/30/2024). The tank was held at a constant temperature of 30 °C until acclimation to experimental vessels occurred on 2/9/2024. Corals were acclimated to experimental conditions four days prior to starting the experiment. Nubbins from this tank were used for treatments exposed to 30 °C (0 NTU and 29 NTU treatments). Nubbins were placed in acclimation vessels (2 L glass beakers filled with ASW) in a temperature-controlled challenge room (27 °C-28 °C). Temperature, salinity, and pH were measured from a random replicate from each treatment during this acclimation period.

2.6. Sediment particle size analysis

Collections of newly-made treatment stocks and treatment solutions just prior to weekly treatment and beaker renewals (referred to as spent treatments) were made

every two weeks to ensure continuity in the turbidity particle size distribution across experiments (see Appx. 6.4.D4 for detailed protocol).

Prior to treatment solution collections, accumulated sediments were lightly-flushed from treatment vessel surfaces (coral and stand) with a plastic transfer pipet to ensure all sediment was properly suspended in the beaker prior to sampling. Approximately 160 mL from replicate beakers were collected by siphoning with a 1/4-inch silicon hose and pooled in a 1 L glass or polypropylene container for a total of ~1 L. For the stock sample, 1 L was pumped from the reservoir into a 1 L bottle. Samples were stored at 4 °C for no longer than one week before processing for sediment particle size analysis.

Samples were taken every other week alternating between treatment change days (Tuesdays and Fridays) for the turbidity dose-response experiment, whereas samples from the dual stressor experiment were collected during both treatment renewal days, every other week. Samples collected from the stock reservoir were mixing for a total of either 3 days (collected Tuesday) or 6 days (collected Friday) whereas samples collected from treatment solutions were mixing for a total of either 6 days (collected Friday) or 10 days (collected Tuesday) from mixing in both the stock reservoir and treatment beakers. The sample collection schedule for each experiment is detailed in **Tables 2 and 3**, respectively.

Table 2. Turbidity treatment sample collection schedule for the turbidity dose-response experiment. Stock and treatment solutions were collected every other week alternating between treatment renewal days. *Note: control treatment samples were not collected.*

Date	Treatment	Days Mixing	Collection Day
9/26/2023	10 NTU	10	Tuesday
9/26/2023	20 NTU	10	Tuesday
9/26/2023	29 NTU	10	Tuesday
9/26/2023	Stock	3	Tuesday
10/13/2023	10 NTU	6	Friday
10/13/2023	20 NTU	6	Friday
10/13/2023	29 NTU	6	Friday
10/13/2023	Stock	6	Friday
10/24/2023	10 NTU	10	Tuesday
10/24/2023	20 NTU	10	Tuesday
10/24/2023	29 NTU	10	Tuesday
10/24/2023	Stock	3	Tuesday
11/10/2023	10 NTU	6	Friday
11/10/2023	20 NTU	6	Friday
11/10/2023	29 NTU	6	Friday
11/10/2023	Stock	6	Friday
11/21/2023	10 NTU	10	Tuesday
11/21/2023	20 NTU	10	Tuesday

11/21/2023	29 NTU	10	Tuesday
11/21/2023	Stock	3	Tuesday
12/8/2023	10 NTU	6	Friday
12/8/2023	20 NTU	6	Friday
12/8/2023	29 NTU	6	Friday
12/8/2023	Stock	6	Friday
12/12/2023	10 NTU	10	Tuesday
12/12/2023	20 NTU	10	Tuesday
12/12/2023	29 NTU	10	Tuesday
12/12/2023	Stock	3	Tuesday

Table 3. Turbidity treatment sample collection schedule for the dual stressor experiment. Stocks and treatment solutions were collected during both treatment renewal days every other week. *Note: control treatment samples were not collected*.

Date	Treatment	Days Mixing	Collection Day
2/13/2024	Stock	3	Tuesday
2/16/2024	Stock	6	Friday
2/16/2024	28 °C/29 NTU (T2)	6	Friday
2/16/2024	30 °C/29 NTU (T4)	6	Friday
2/27/2024	Stock	3	Tuesday
2/27/2024	28 °C/29 NTU (T2)	10	Tuesday
2/27/2024	30 °C/29 NTU (T4)	10	Tuesday
3/1/2024	Stock	6	Friday
3/1/2024	28 °C/29 NTU (T2)	6	Friday
3/1/2024	30 °C/29 NTU (T4)	6	Friday
3/12/2024	Stock	3	Tuesday
3/12/2024	28 °C/29 NTU (T2)	10	Tuesday
3/12/2024	30 °C/29 NTU (T4)	10	Tuesday
3/15/2024	Stock	6	Friday
3/15/2024	28 °C/29 NTU (T2)	6	Friday
3/15/2024	30 °C/29 NTU (T4)	6	Friday
3/26/2024	Stock	3	Tuesday
3/26/2024	28 °C/29 NTU (T2)	10	Tuesday
3/26/2024	30 °C/29 NTU (T4)	10	Tuesday
3/29/2024	Stock	6	Friday
3/29/2024	28 °C/29 NTU (T2)	6	Friday
3/29/2024	30 °C/29 NTU (T4)	6	Friday
4/9/2024	Stock	3	Tuesday
4/9/2024	28 °C/29 NTU (T2)	10	Tuesday
4/9/2024	30 °C/29 NTU (T4)	10	Tuesday

4/12/2024	Stock	6	Friday
4/12/2024	28 °C/29 NTU (T2)	6	Friday
4/12/2024	30 °C/29 NTU (T4)	6	Friday
4/23/2024	Stock	3	Tuesday
4/23/2024	28 °C/29 NTU (T2)	10	Tuesday
4/23/2024	30 °C/29 NTU (T4)	10	Tuesday
4/26/2024	Stock	6	Friday
4/26/2024	28 °C/29 NTU (T2)	6	Friday
4/26/2024	30 °C/29 NTU (T4)	6	Friday
5/7/2024	Stock	3	Tuesday
5/7/2024	28 °C/29 NTU (T2)	10	Tuesday
5/7/2024	30 °C/29 NTU (T4)	10	Tuesday

Each treatment solution was processed by dividing the 1 L equally into four 250 mL polypropylene centrifuge bottles and centrifuged (Avanti J-20 XPI, Beckman Coulter) at 7500 rpm (10,395 *x g*) for 30 min at 20 °C in a swinging bucket rotor (JS-7.5, Beckman Coulter). The supernatant was decanted, leaving ~75 mL in each of the four bottles. The pellets were resuspended by vortexing at the maximum setting for 10 sec and the contents (approx. 300 mL total) were equally transferred into six 50 mL polypropylene Falcon tubes (Fisher Scientific, Hampton, NH). Sediment concentrates were centrifuged at 5000 rpm (4620 *x g*) for 30 min at 20 °C using the JS-7.5 swinging bucket rotor and adaptors. [The use of 4620 *x g* was more than twice the centrifugal force used by similar extraction protocols (Anschutz & Charbonnier, 2021) and was used to capture the greatest range of particle sizes.]

The supernatant was decanted leaving only the pelleted sediment. Residual salt, which can interfere with the downstream particle analysis, was removed by adding 40 mL of Type I water to one of the six tubes, shaken briskly to dislodge the pellet, and poured into one of the remaining five tubes. This sequence was repeated with the remaining tubes, leaving one tube containing 40 mL of Type I water with all sediment concentrated. The contents were then split between two 50 mL tubes (20 mL each) and centrifuged at 5000 rpm (4620 *x g*) for 30 min at 20 °C. The supernatant was decanted and 15 mL of Type I water was added to one of the two tubes and vortexed at the maximum setting for 10 sec to resuspend the pellet. The contents of this tube were combined with the second tube which was vortexed on the maximum setting for 10 sec to resuspend the pellet. This was then poured into a circular aluminum weigh dish (Fisher Scientific, Hampton, NH). The sediment solution was then dried at 100 °C overnight. The next day, the dried sediment was transferred into 1.5 mL Eppendorf tube using a small brush and stored at 4 °C until for particle size analysis, typically within 30 days. A Malvern Mastersizer 3000 (Malvern, United Kingdom) (range: 0.01 – 3500 µm) was used to determine the particle size distribution of sediment in the stock and treatment solutions (see Appx. 6.4.D4 for details).

2.7. Algal symbiont responses

2.7.1. Maximum quantum yield (Fv/Fm)

Algal symbiont chlorophyll *a* fluorescence was measured as previously described (Ralph et al. 2005; May et al. 2020). Briefly, ~30-45 min before the end of the dark cycle, sediment was removed from corals (as described in section 2.4.1) using a 3 mL disposable pipette, and nubbins were placed in a custom Teflon stand in ASW in a clean glass crystallizing dish. Dark conditions were maintained by carrying out procedures under green light (headlamps). *[Green light is reflected and absorbed the least by the algae, thus maintains the photosynthetic dark cycle while not triggering the photosynthetic light cycle.]* Images and data were collected using an Imaging PAM M-series chlorophyll fluorometer (MAXI version, Walz GmbH, Effeltrich, Germany). An area of interest from the top of each coral nubbin near the center was selected from each image, with care to avoid the wounded area prior to starting the tissue regeneration assay (see Appx. 6.4.D5 for details).

2.7.2. Dinoflagellate symbiont density measurements

The density of dinoflagellate symbionts was determined from histological sections that were subsampled from control and experimental nubbins at the termination of the experiment. Tissue samples were subsampled using a Gryphon C-40 Diamond Band Saw in a dry mode (i.e., without a steady stream of ASW) and after a 48-h recovery period for handling during measurement to reduce possible stress artifacts. One of the subsamples was fixed in 1:4 zinc-formalin (5x Z-fix concentrate, Anatech Ltd., Battle creek MI) in artificial seawater for 24 h. Tissues then were photographed and excess fixative was rinsed from the samples in 0.2 µm-filtered artificial seawater. Samples were fully decalcified (approximately 1-3 weeks) using 0.5 M EDTA (pH 7.0, adjusted with HCl once Na_2EDTA is dissolved). Tissues were dehydrated in a series of ethanol dilutions (50, 60 and 70%) and processed in an automatic tissue processor before embedding in paraffin. Paraffin blocks were sectioned (to include a sagittal plane) at a 4 µm thickness and slides stained with hematoxylin and eosin.

Photomicrographs of 10 fields of view were randomly captured throughout the polyp surface body wall from each experimental replicate at 40x magnification. The gastrodermal tissue was digitally isolated from photomicrographs of the resulting stained slides representing each experimental nubbin using the lasso tool in Adobe Photoshop. The area (μm^2) of the gastrodermis was measured using ImageJ image processing software. Total algal symbiont density was calculated using the ImageJ cell counter plugin (RRID:SCR 003070). The total number of algal cells was divided by the area of gastroderm in each of the 10 images to obtain a final number of dinoflagellate cells per μm^2 of gastrodermal tissue. The average dinoflagellate density for each coral replicate was calculated by averaging the cell numbers across the 10 replicate micrographs resulting in a final measurement of algal symbiont cells per μm^2 of gastrodermal tissue (see Appx. 6.4.D6 for details).

2.8. Coral responses

2.8.1. Growth measured as calcium carbonate deposition

Measurements for coral buoyant weight were collected weekly throughout the 90-day experiment according to methods outlined in Dodge et al. (1984). Briefly, the coral nubbins were suspended in 2 L of artificial seawater from the underhook of a milligram analytical balance. Calibration verification was performed using a 10 g NIST standard each week prior to buoyant weight measurement collection. The gross buoyant weight was recorded for each coral sample attached to a Teflon support peg. To account for the weight of the peg, an average buoyant weight was obtained from five pegs not used in the experiment (1.887 g) and this value was subtracted from the gross buoyant weight of each coral sample. Temperature and salinity from the artificial seawater used to measure buoyant weight were also recorded to calculate seawater density using tables from Bialek (1966). Buoyant (wet) weight can be converted to dry weight based on seawater density derived from the temperature, salinity and using aragonite density of 2.94 g cm^{-3}. Net growth of coral nubbins was determined based on the buoyant weight technique of Jokiel et al. (1978). The change in dry weight can be used to calculate growth rate (calcification), and percentage of growth over the duration of the exposure when compared to controls. Dry weight at each time point was compared to respective time 0 measurements to calculate percent growth (see Appx. 6.4.D7 for details).

2.8.2. Tissue regeneration

Previous work has shown that *O. faveolata* nubbins under the control conditions used in this project, will heal within two weeks. Due to the duration of turbidity exposure the tissue regeneration assay was conducted the final two weeks (following 76 days of turbidity exposure) of the experiment. Lacerations were created at the top of each *O. faveolata* nubbin by removing them from the exposure vessel and placing the nubbin in a Dremel workstation, approximately 2 cm below a Dremel rotary tool fitted with a 2.0 mm diamond hole saw bit (Lasco Diamond Products, Los Angeles, CA). Coral support pegs were held in place manually. The drill bit was lowered onto the coral surface over the center of a polyp and the tissue removed to a depth of approximately 2 mm, removing a single poly. The wound was cleaned of tissue debris by gently flushing the area with ASW using a 1000 µL micropipettor.

Immediately after wounding, buoyant weight was measured from each nubbin (detailed in section 2.8.1), and were then placed in a 500 mL crystalizing dish filled with fresh ASW until all replicates within a treatment (n = 6) were wounded and weighed. Coral nubbins from each treatment were then imaged under brightfield and fluorescence using a MVX10 research macro zoom microscope (detailed in section 2.4.1 and Appx. 6.4.D8) (filter #U-MWB2; filter #U-MNV2: excitation: 400-410 nm; emission (barrier filter): 455 nm; dichromatic mirror: DM400-410; Chroma Technology Corp, Bellows Falls, VT). Photomacrographs of wounds were collected by placing a centimeter ruler next to the laceration. While brightfield images provide visualization of tissue margins, fluorescent images (under wide blue and narrow violet wavelengths) excite green fluorescent protein in coral tissue, which allows more accurate measurement for tissue regeneration assays. Images of wounds were captured daily following wounding for two weeks. Skeletal area for each coral image was determined using ImageJ freehand tool (Schneider et al. 2012) and a modified macro (pixel units were calibrated to cm) from the NOAA/NCCOS Coral Disease and

Health Consortium website (https://cdhc.noaa.gov/education/coral_assay.aspx; macro is provided as Appx. 6.3C). Total area of bare skeleton and wound perimeter values were recorded for each fragment at time 0 and daily images. Percent tissue regeneration was determined from the difference in skeletal area between the time 0 and the experimental time points. Skeletal area measurements from each nubbin were compared to each experimental timepoint to calculate percent tissue regeneration over time (see Appx. 6.4.D8).

2.9. Energy reserves

2.9.1. Total lipid and total soluble protein

Following homogenization of each coral nubbin (tissue and skeleton) using a cryomill (RETSCH 207490001 Cryomill, Haan, Germany) and lyophilization (Labconco FreeZone, Kansas City, MO), a modified SIMPLEX method (Coman et al. 2016) was used to extract total lipids and total soluble protein. For simultaneous lipid and protein extraction, cold methanol (MeOH) was added to each sample of lyophilized coral powder, which was then repeatedly (3x) vortexed, incubated in liquid nitrogen (30 s), thawed at room temperature, and sonicated (10 min). Cold methyl tert-butyl ether was added to samples and incubated for 1 h at 4 °C under constant agitation. Phase separation was induced with the addition of Type 1 water containing 0.1 % ammonium acetate and centrifuging (10 min at 1,000 *x g*). The upper organic phase containing lipids was removed using a glass pipet, dried under vacuum and then quantified gravimetrically on a semi microbalance.

Proteins were isolated using the following steps: 1) protein precipitation (MeOH was added to the lower aqueous phase in a final ratio of 4:1, v/v MeOH/water, samples were incubated overnight at -20 °C and then centrifuged for 12 min at 5,000 *x g* at 4 °C); 2) protein denaturation (freshly prepared denaturing buffer and a mixture of 6-aminocaproic acid (5 mM), benzamidine (200 mM), phenylmethylsulfonyl fluoride (200 mM) and 0.01 % protease inhibitor cocktail (stored in 50 % glycerol) were added to the samples, which were then repeatedly incubated at 90 °C (3 min) and vortexed two times before being centrifuged for 15 min at 20,000 *x g*); and 3) soluble protein fraction was removed and protein concentration quantified using a Pierce bicinchoninic acid assay (ThermoFisher Scientific, Cat. # 23225).

Analyses of total soluble proteins and total lipids were performed after normalizing protein and lipid mass (grams) to estimated tissue mass (grams) from the homogenate powder used per sample, which was calculated using an average ash-free dry weight of *O. faveolata*. Estimated tissue mass was also determined by drying the skeletonal remains following lipid and protein extraction and subtracting the organic-free skeleton mass from the initial mass (tissue and skeleton). This was completed by treating skeleton with 1 mL 10 % sodium dodecyl sulfate and vortexing (3x) before placing in a 56 °C incubator overnight. The next day, samples were centrifuged (3000 x g for 10 min at 4 °C) and supernatant was collected. A 1000 µL pipette was used to add ~1 mL MeOH to the skeleton particulate to further digest any organic matter remaining and transfer skeleton particulate to labeled/weighed tubes. Samples were placed in a 56 °C incubator to evaporate MeOH until samples were completely dry (at

least three days). These processes were completed for experimental coral nubbins and time-0 nubbins, which were a baseline for biochemical analyses (see Appx. 6.4.D9 for details).

2.9.2. Triglyceride lipid assay

Triglyceride concentration was calculated using the triglyceride (TG) colorimetric assay kit (Invitrogen, Thermo Fisher Scientific, Inc.) for the 90-day dual stressor experiment. Coral powder (100 mg) was resuspended in 4.5 mL of anhydrous ethanol. Once mixed, samples were centrifuged at 1500 x *g* for 10 min at 4 °C to pellet the skeleton and protein. The supernatant was removed and pipetted into a 96-well assay plate. From here, all kit instructions were followed and TG was calculated according to the given formula. Tissue mass was estimated from dry skeleton particulate mass after TG extraction by subtracting the dry skeleton mass from the initial powder mass (process detailed in section 2.9.1). These processes were completed for experimental coral nubbins and time-0 nubbins, which were a baseline for biochemical analyses (see Appx. 6.4.D10 for details).

2.10. Statistical analyses

2.10.1. 90-day turbidity dose response experiment

All analyses for the turbidity dose-response (0, 10, 20, and 29 NTU) experiment, with *O. faveolata* nubbins were conducted using RStudio, version 4.3.2. All endpoints that were measured over time (maximum quantum yield and change in dry weight measured weekly, percent tissue regeneration measured daily near the experiment end) were analyzed using a repeated measures ANOVA followed by Tukey's posttest if parameters were met and a nonparametric ANOVA with rank transformed data followed by pairwise comparisons using paired t-tests if they were not met to test for overall effects, and a mixed-model to test for effects over time. All terminal measurements collected on the final day of the experiment (maximum quantum yield (Fv/Fm), gain in dry weight, percent increase in calcium carbonate deposition, total soluble proteins/ lipids, symbiont density within the gastrodermis, and percent tissue regeneration) were analyzed using one-way ANOVA followed by Tukey's posttest if parametric assumptions were met and a non-parametric Kruskal-Wallis test followed by a Dunn's posttest if assumptions were not met. Particle size analysis was performed using GraphPad Prism, version 10.0.3. If ANOVA assumptions were not met, a non-parametric (Kruskal-Wallis) test was performed with Dunn's posttest.

2.10.2. 90-day dual stressor experiment

All analyses for *O. faveolata* endpoints in the turbidity (0 and 29 NTU) and temperature (28 °C and 30 °C) dual stressor experiment were conducted using RStudio, version 4.3.2. All endpoints that were measured over time (maximum quantum yield and change in dry weight measured weekly, percent tissue regeneration measured daily near the experiment end) were analyzed using a two-way repeated measures ANOVA followed by Tukey's posttest if parameters were met and a nonparametric ANOVA with rank transformed data followed by pairwise comparisons using paired t-tests if the assumptions were not met for the ANOVA to

test for overall effects. A mixed-model was used to test for effects over time. All terminal measurements collected on the final day of the experiment (maximum quantum yield (Fv/Fm), gain in dry weight, percent increase in calcium carbonate deposition, total soluble proteins/lipids, symbiont density within the gastrodermis, and percent tissue regeneration) were analyzed using a two-way ANOVA followed by Tukey's posttest if parametric assumptions were met and a non-parametric Kruskal-Wallis test followed by a Dunn's posttest if the assumptions were not met. Particle size analysis (one-way ANOVA with Tukey's multiple comparisons test) was performed using GraphPad Prism, version 10.0.3.

3. RESULTS AND DISCUSSION

3.1. Particle size analysis

The average particle size of sediment used in this project were similarly-sized with an average grain size of 23.6 µm across both the dose-response and dual stressor experiments (**Table 4**).

Table 4. Mean particle sizes (Dv50 in µm) in the dose-response and dual stressor experiments. Dv50 is the mean particle size and SD is standard deviation.

Experiment	Treatment	Dv50 (µm)	SD
Dose-response	10 NTU	30.6	3.5
Dose-response	20 NTU	21.4	1.1
Dose-response	29 NTU	20.4	4.7
Dose-response	Stock	19.9	3.8
Dual stressor	28 °C/29 NTU (T2)	24.7	2.3
Dual stressor	30 °C/29 NTU (T4)	25.2	2.6
Dual stressor	Stock	23.2	3.5
	Mean	23.6	

Dv50 values provide the median particle size for the volume distribution in a sample (Burgess et al. 2004) which consistently ranged between 14-38 µm (**Figures 2-5**). The majority of sediment particles were Wentworth sediment size classified as silts (Wentworth 1922).

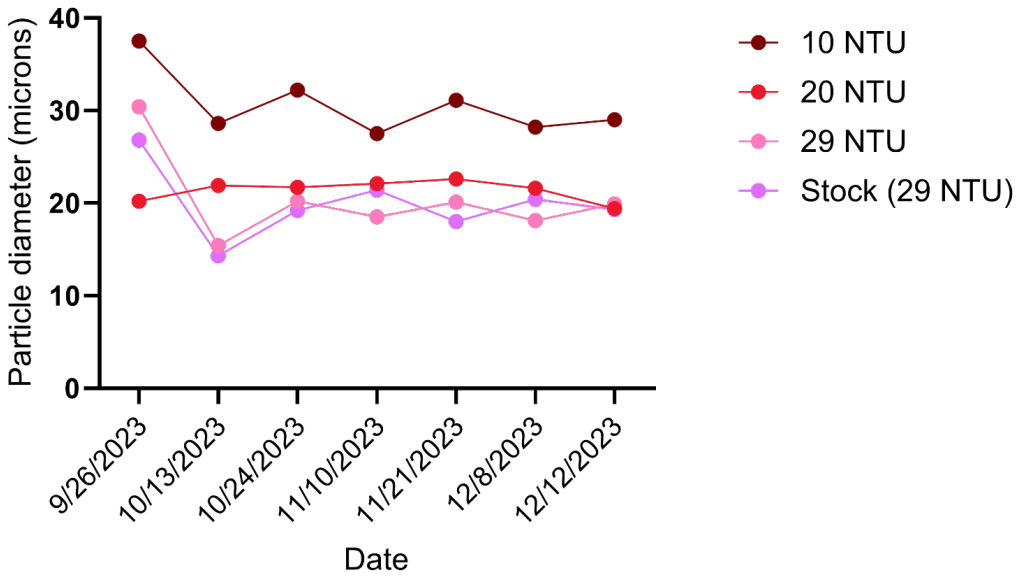

Figure 2. Mean particle size (Dv50 values, in µm) from particle size analysis over time in the dose-response experiment. Treatment particle sizes: 10 NTU (maroon line) ranged from 27-38 µm; 20 NTU (red line) ranged from 20–23 µm; 29 NTU (pink line) ranged from 15–30 µm; stock solutions (purple line) ranged from 14-27 µm.

In the dose response experiment, a significant difference ($p<0.05$) in the DV50 particle size was found between the 10 NTU treatment and the stock and 29 NTU treatment (**Figures 2 and 3**). The mean Dv50 particle size of the 10 NTU treatment was significantly larger than that of the 20 and 29 NTU treatments, which were not significantly different from each other **(Figures 2 and 3)**. As in the dose response experiment, the 29 NTU mean particle sizes were not significantly different in the dual stressor experiment between temperature groups (**Figures 4 and 5**).

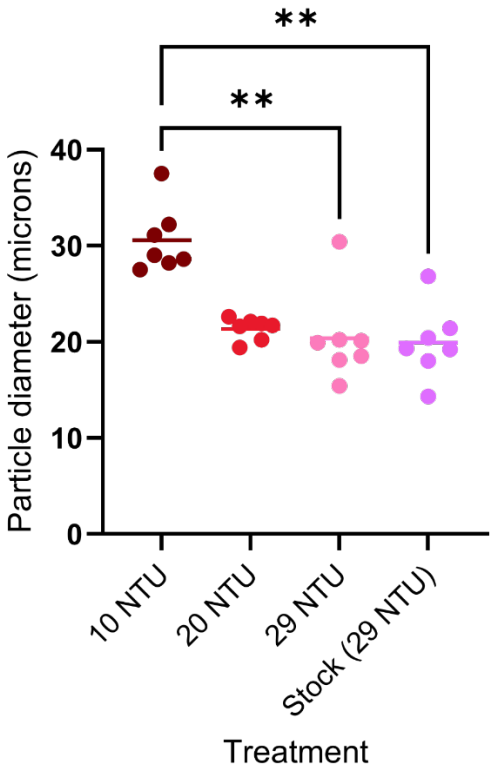

Figure 3. Comparison of Dv50 particle sizes (in µm) in the dose-response experiment. A significant difference (Kruskal-Wallis, $p<0.05$) was found between treatments, with particles in the 10 NTU treatment larger than those in the 29 NTU treatments or stock solution.

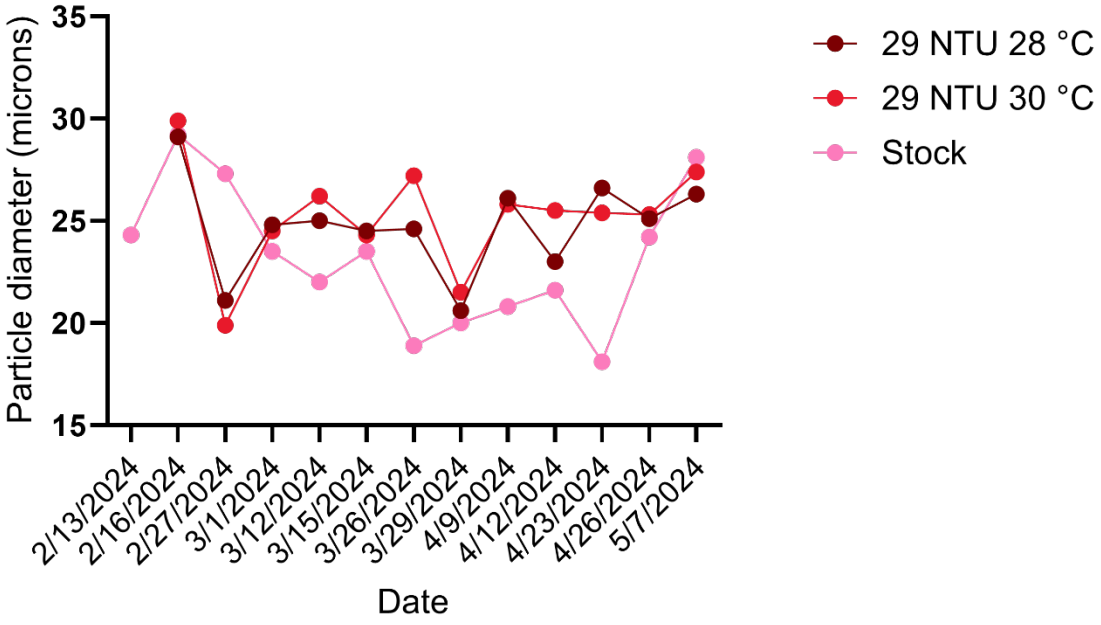

Figure 4. Dv50 values (in µm) from the particle size analysis over time in the dual stressor experiment. Sediment particle sizes: 29 NTU/28 °C (maroon line) ranged from 20-29 µm; 29 NTU/30 °C (red line) ranged from 20–30 µm; stock solution (purple line) ranged from 18-29 µm.

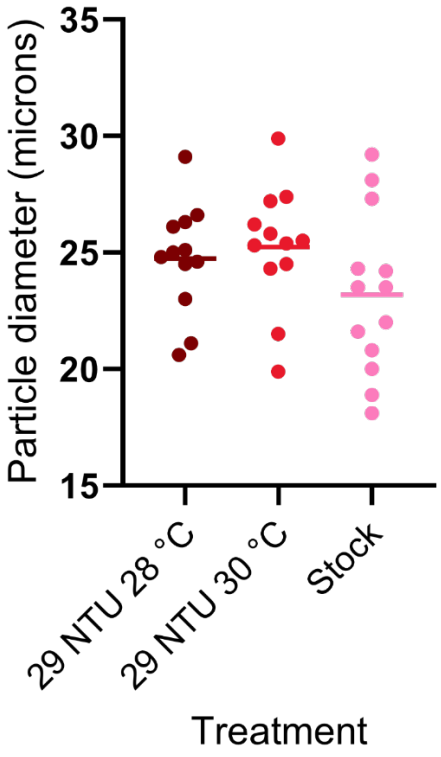

Figure 5. Comparison of Dv50 particle sizes (in µm) in the dual stressor experiment. No significant differences (one-way ANOVA) were found between treatments 28 °C/29 NTU and 30 °C/29 NTU or the stock solution.

3.2. 90-day turbidity dose-response experiment

3.2.1. Water quality

Water quality parameters maintained stable levels throughout the experiment with temperature, salinity, and pH remaining consistent across treatments (**Table 5**).

Temperature was consistent between treatment groups and stayed within a range of 1.6 °C (27.1-28.7 °C) throughout the course of the experiment (**Figure 6A**). After treatment renewal, (noted as "Fresh" on the graph x-axis), the temperature did drop temporarily in treatment groups of 0 and 10 NTU, however the temperatures returned to 28 °C by the measurement on the following day. This is likely due to the location of the 0 and 10 NTU stock solutions and the variable air flow pattern within the experimental room. Because the temperature quickly stabilized between all treatment groups, this is not believed to have any impact on the experiment results.

The pH was consistent throughout the study, with the 0 NTU treatment slightly higher than the other three treatment groups (**Figure 6B**). The pH temporarily increased in all treatment groups after treatment renewals (noted as "po"), likely as a

result of removing byproducts of cellular respiration (CO_2) generated within the treatment vessel between treatment changes.

Salinity remained stable throughout the study, with the exception of a slight decrease on Oct 13 and 17, 2023 (**Figure 6C**). However, all samples experienced a similar salinity decrease to ~35 ppt, which is still within optimal thresholds for corals, so any effects should be negligible to this study. Salinity maintained a range of 1.9 ppt throughout the experiment and was not affected by treatment renewals (noted on the graph axis as "Spent" and "Fresh" to indicate the type of treatment measured in regards to the treatment change).

Turbidity maintained targeted levels measured in NTU. The target NTUs of 0, 10, 20, and 29 were consistently achieved within each respective treatment vessel throughout this study (**Figure 6D**). There were consistent decreases in NTU in each group prior to the sediment being resuspended (pre), but after sediment was resuspended, the targeted NTUs were achieved (po). The result of the water quality measurements (temperature, pH, salinity, and turbidity) showed that there was no significant unintended variability in any of these parameters that would have influenced the results of either of these studies.

Table 5. Descriptive statistics for water quality measurements collected throughout the 90-day turbidity dose-response experiment (0, 10, 20, 29) with *O. faveolata*. Turbidity statistics are calculated from daily maximum measurements. SD is standard deviation from the mean.

	0 NTU	**0 NTU**	**10 NTU**	**10 NTU**	**20 NTU**	**20 NTU**	**29 NTU**	**29 NTU**
Parameter	Mean	SD	Mean	SD	Mean	SD	Mean	SD
Temperature (°C)	27.982	0.2433	28.086	0.2524	28.028	0.255	27.952	0.2803
Salinity (ppt)	36.2641	0.39249	36.4685	0.3786	36.164	0.35326	36.1656	0.38816
pH	7.94839	0.10501	7.88981	0.102	7.87284	0.10671	7.83923	0.09422
Turbidity (NTU)	0.5271	0.1267	10.346	0.857	20.452	0.9442	29.533	0.9934

A.

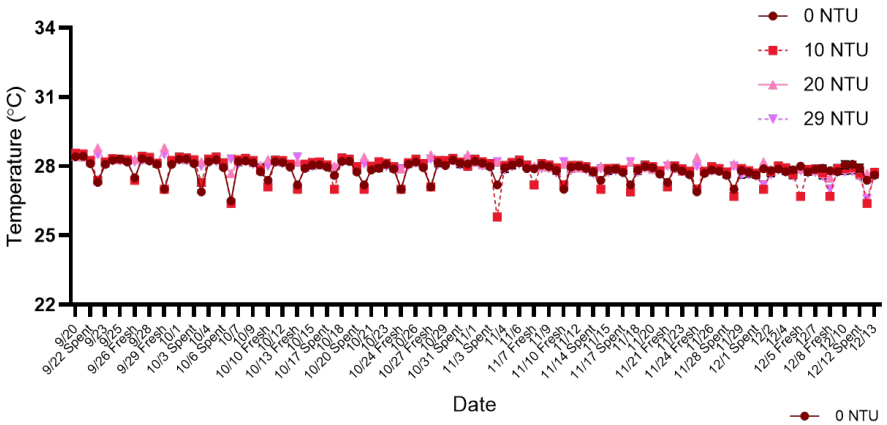
0 NTU
10 NTU
20 NTU
29 NTU
Temperature (°C)
34
31
28
25
22
Date

B.

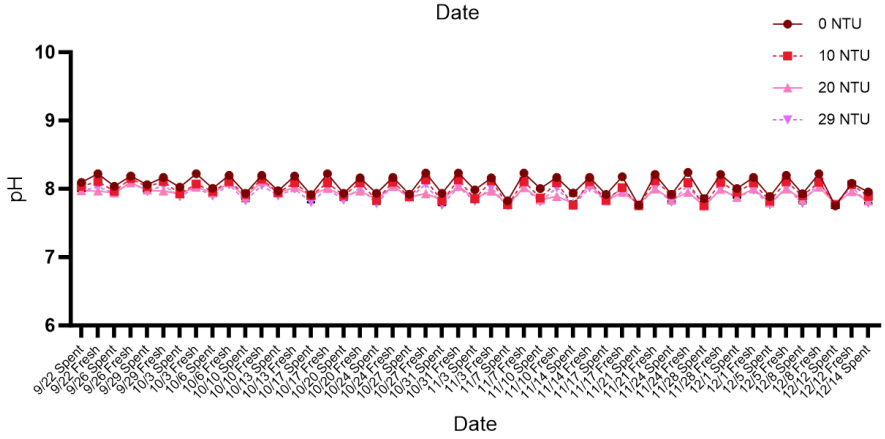
0 NTU
10 NTU
20 NTU
29 NTU
pH
10
9
8
7
6
Date

C.

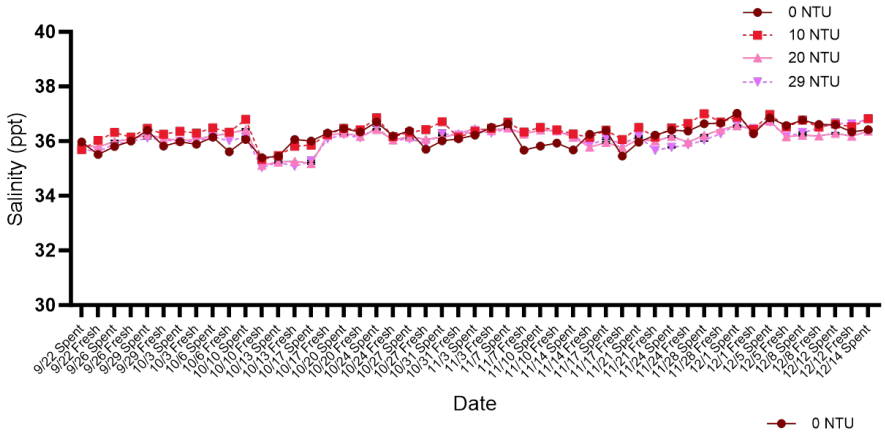
0 NTU
10 NTU
20 NTU
29 NTU
Salinity (ppt)
40
38
36
34
32
30
Date

D.

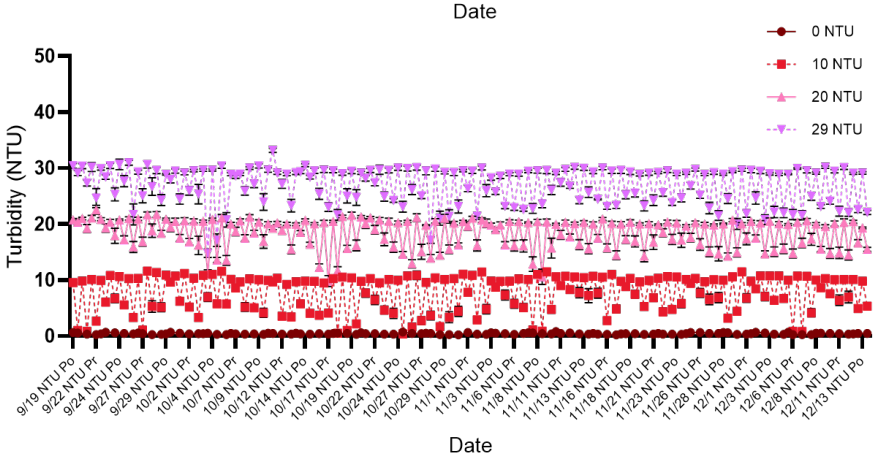
0 NTU
10 NTU
20 NTU
29 NTU
Turbidity (NTU)
50
40
30
20
10
0
Date

Figure 6. Water quality measurements collected throughout the 90-day turbidity dose-response experiment of targeted turbidity levels 0, 10, 20, and 29 NTU. **A)** Average daily temperature (°C) and daily measurements from "Fresh" and "Spent" treatments were collected at treatment renewals: **B)** average pH; **C)** average salinity (ppt); **D)** average daily turbidity (NTU) labeled "Pr" and "Po" indicating measurements before (pre) or after (post) sediment resuspension from nubbins and beakers. Error bars represent standard error of the mean.

3.2.2. Effect of turbidity exposure on photosynthetic efficiency of *O. faveolata* algal symbionts

The photosynthetic efficiency (measured as dark-adapted maximum quantum yield, or Fv/Fm, **Figure 7**) of coral nubbins in all tested turbidities (10, 20, and 29 NTU) were significantly higher than those measured in the 0 NTU control group over time ($p = 0.0017$, nonparametric ANOVA with rank transformed data, **Figure 8A**). In the final Fv/Fm reading taken at the experiment end, only the fragments in the highest turbidity treatment (29 NTU) still had a significantly greater photosynthetic efficiency than the 0 NTU control group ($p = 0.0011933$, ordinary one-way ANOVA, **Figure 8B**), suggesting that the lower turbidity groups began to exhibit Fv/Fm comparable to the 0 NTU group by the end of the 90-day experiment duration. It is possible that the positive relationship between the photosynthetic efficiency of *O. faveolata* symbionts (in this experiment known to be *Cladocopium* sp.) with increasing turbidities may be due to increased light diffusion (~5% decrease in PAR observed at 29 NTU in experimental conditions), and/or increased nutrient availability (i.e., organic matter associated with sediment) in the turbid conditions. The maximum quantum yield (Fv/Fm) of all test nubbins stayed within a normal range (~0.6) throughout the experiment (**Figure 8C**).

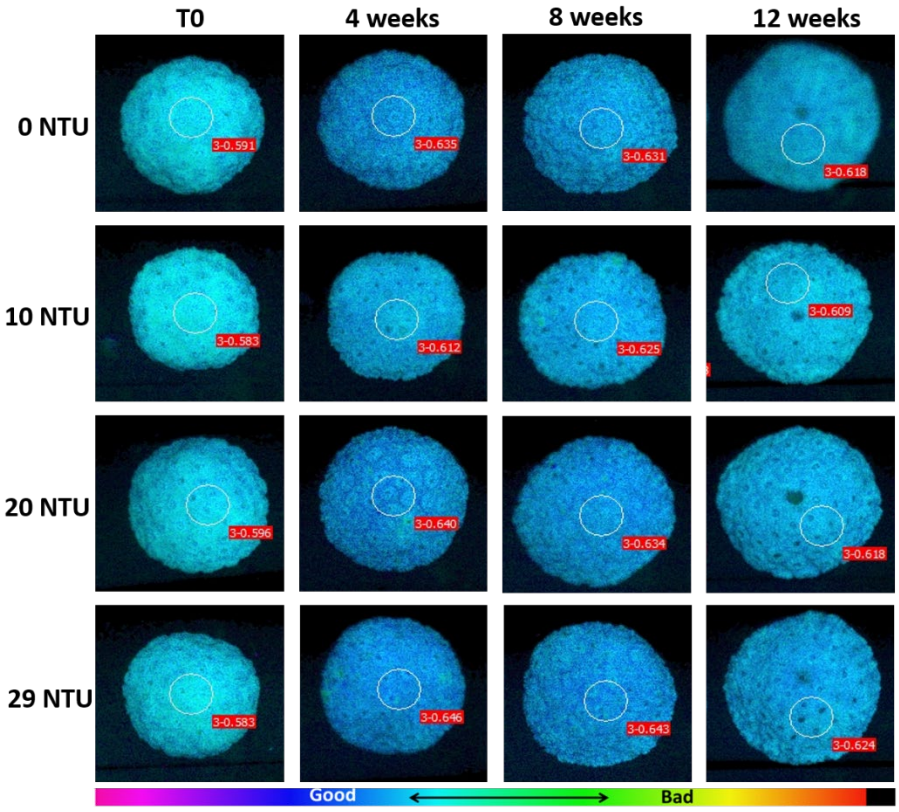

Figure 7. Representative pulse amplitude modulated (PAM) fluorometry images of *O. faveolata* nubbins used in the 90-day turbidity dose-response experiment. Chlorophyll *a* fluorescence images are of the same coral nubbin in each turbidity exposure (0, 10, 20, and 29 NTU) over time. Images from week 12 show the healing wound used in the tissue regeneration assay (dark area in center of images). The white circles on each image represent the area of interest used to measure Fv/Fm (values in the red box on each image). A heat map below the image grouping shows the relative color with respect to chlorophyll *a* fluorescence, with blue colors indicating higher fluorescence and red indicating lower fluorescence.

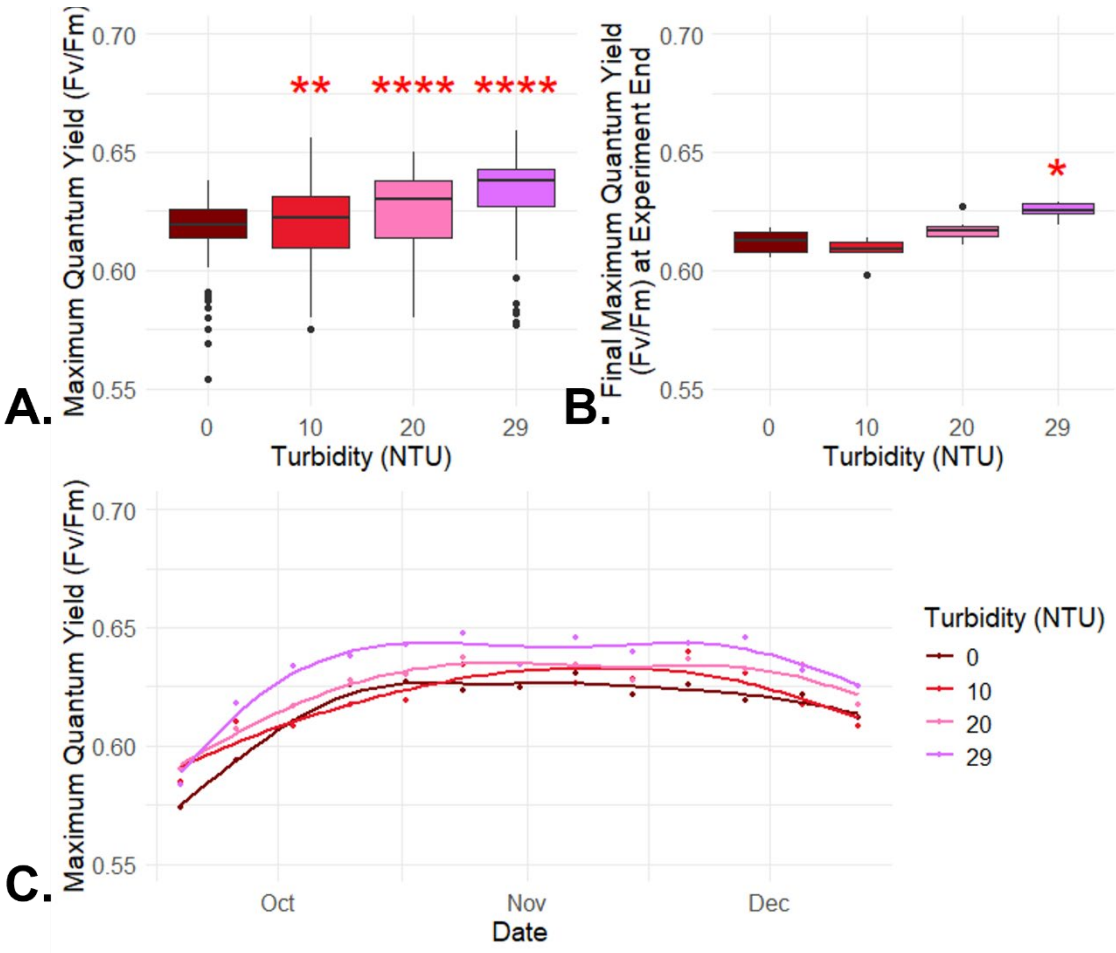

Figure 8. Maximum quantum yield (Fv/Fm) of *O. faveolata* nubbins in a 90-day dose-response to turbidity. **A)** A box and whisker plot showing the repeated measures Fv/Fm data of each treatment over the 90-day experiment. The photosynthetic efficiency in all tested turbidity groups (10, 20, 29 NTU) was significantly higher than in the 0 NTU control group ($p=0.01$, $p<0.0001$, $p<0.0001$, respectively, pairwise comparisons using paired t-tests. **B)** Final measurements of Fv/Fm of each treatment taken at the experiment end. Only the nubbins in the highest turbidity treatment (29 NTU) still had a significantly higher Fv/Fm than those in the 0 NTU control ($p=0.0012$, one-way ANOVA with Tukey's multiple comparisons). **C)** Weekly averages of maximum quantum yield (Fv/Fm) in each treatment group over the course of the experiment. A smooth curve fitted with a generalized additive model (GAM) is shown for each turbidity condition to highlight trends over time. Turbidity did not have any effect on changes in Fv/Fm over time ($p>0.05$, linear mixed-effects model).

3.2.3. Effect of turbidity exposure on *O. faveolata* algal symbiont density

Turbidity as high as 29 NTU had no significant effect on the density of algal symbionts (*Cladocopium* sp.) within the gastrodermis of *O. faveolata* fragments after 90 days ($p = 0.1406$, one-way ANOVA, **Figure 9**). This lack of effect may be partly a result of the symbionts themselves rather than of the coral host. Certain species of *Cladocopium* sp. have been found to be well-adapted to various habitats (e.g., light intensities)

(LaJeunesse et al. 2018; Saad et al. 2022), thus changes in turbidity, and therefore light conditions, would not be expected to have adverse effects on symbiont density.

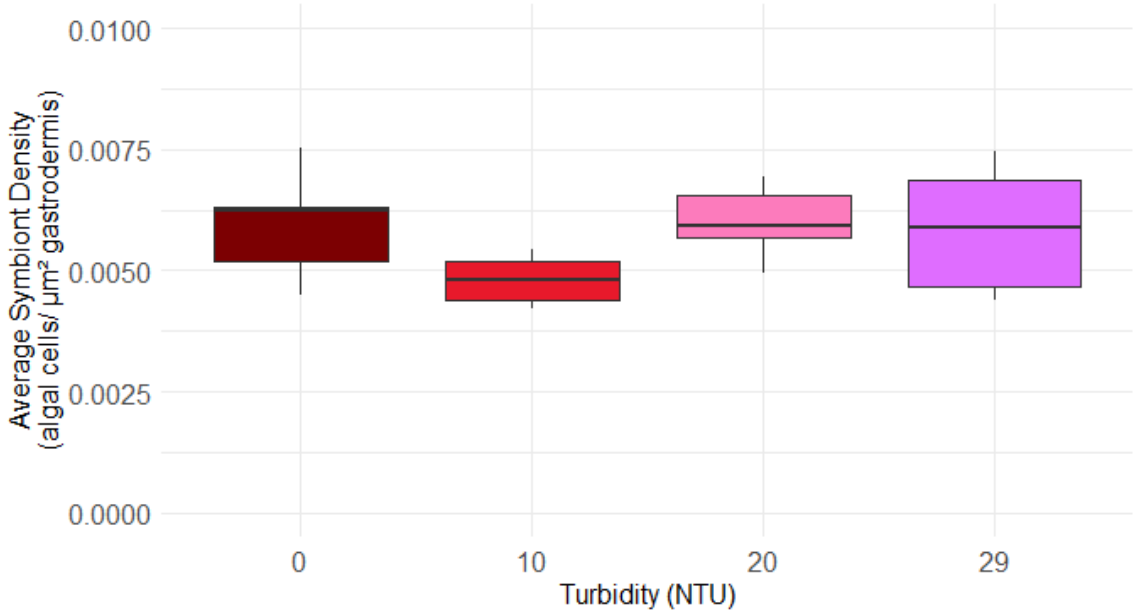

Figure 7. Average dinoflagellate cells per µm^2 of gastrodermal tissue in corals after the 90-day turbidity dose response experiment (0, 10, 20, and 29 NTU). There was no significant difference between treatment groups (p = 0.1406, one-way ANOVA).

3.2.4. Effect of turbidity exposure on coral growth

Turbidity as high as 29 NTU had no significant impact on the growth (measured as percent increase in calculated dry weight) (p=0.6426, nonparametric ANOVA using rank transformed data, **Figure 10 A, B**) or on the growth rate (p>0.05, linear mixed effects model, **Figure 10C**) of *O. faveolata* nubbins over the course of the 90-day experiment. All of the test nubbins grew consistently with weight gains around 1.5 g for all nubbins, reflecting a 27-31% weight increase over the course of the 90 days (**Figure 10C**).

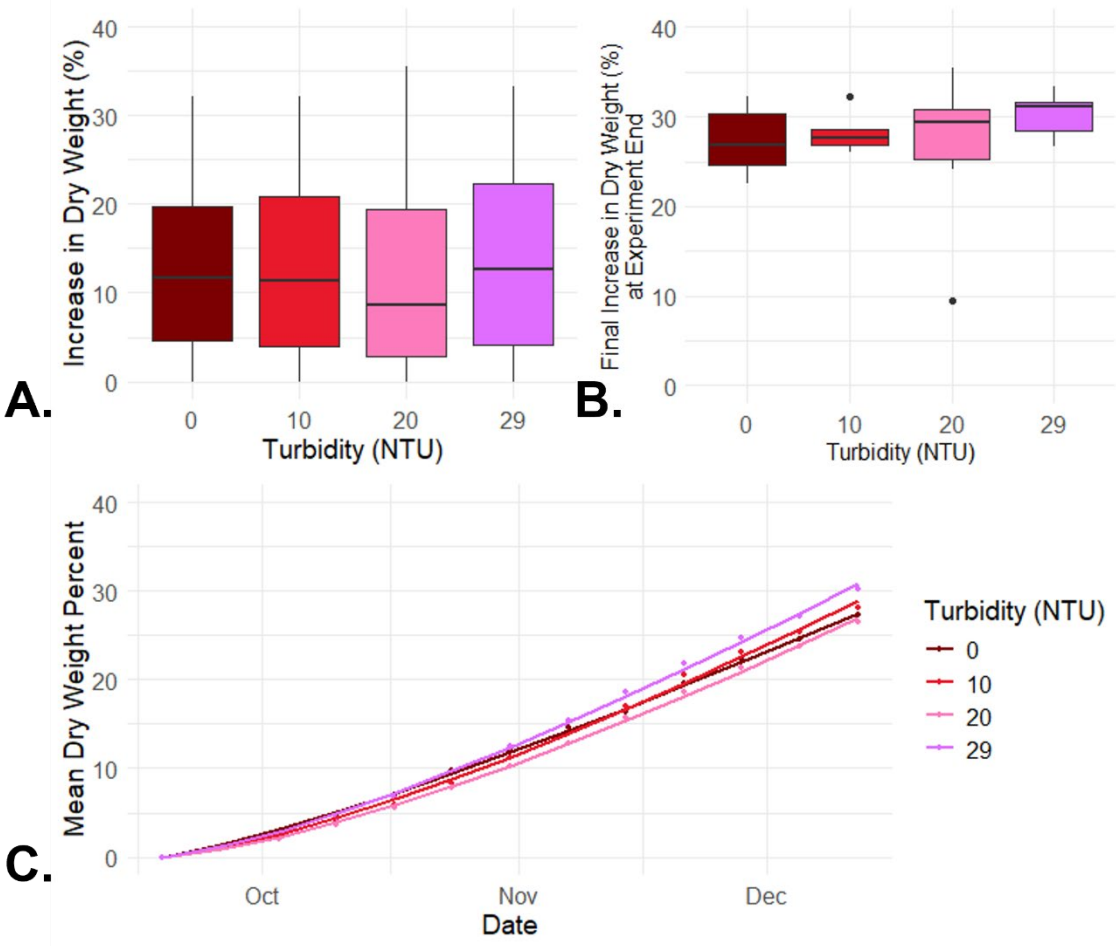

Figure 8. Change in dry weight of corals after a 90-day turbidity dose-response (0, 10, 20, and 29 NTU) experiment. **A**) A box and whisker plot showing the repeated measures dry weight (%) data of each treatment over the 90-day experiment. There was no significant difference between the growth of nubbins in any turbidity treatment compared with those in the 0 NTU control group ($p=0.6426$, nonparametric ANOVA using rank transformed data). **B**) Final measurements of dry weight (%) of nubbins in each treatment taken on the last day of the experiment. There was no significant difference between the total increase in dry weight after 90 days of nubbins in any turbidity treatment compared with those in the 0 NTU control group ($p=0.6385$, ordinary one-way ANOVA). **C**) Weekly averages of dry weight gain (%) in each treatment group over the course of the experiment. A smooth curve fitted with a power model using the nonlinear least squares method is shown for each turbidity condition to highlight trends over time. Turbidity had no effect on changes in growth rates over time ($p<0.05$, linear mixed effects model).

3.2.5. Effects of turbidity exposure on coral tissue regeneration

Turbidity had a significant negative effect on the wound healing capabilities of *O. faveolata* ($p=0.0148$, non-parametric ANOVA using rank transformed data, **Figure 11**). All turbidity treatments (10, 20, 29 NTU) had significantly lower percentages of regenerated tissue ($p=0.01$, $p<0.0001$, $p<0.0001$, respectively, pairwise comparisons using paired t-tests, **Figure 11A**) and a significantly slower rate of tissue regeneration

($p=0.0256$, $p<0.0001$, $p<0.0001$, respectively, linear mixed-effects model, **Figure 11C**) than the 0 NTU control over the course of the 14-day healing period. A non-linear mixed effects model was used to determine the xmid (time point in the healing process in which the mean regenerated tissue was 50 %) for each treatment group and showed that coral healing was delayed for all turbidity treatments: 10 NTU = 2.6-day delay, 20 NTU = 5-day delay and 29 NTU = 4.4-day delay (**Figure 11C**). However, when considering only the final measurement of regenerated tissue taken at the experiment end, there was no difference between any of the treatment groups, indicating that the difference in regeneration caused by turbidity is overcome by 14 days post wounding ($p<0.05$, Kruskal-Wallis test with Dunn's multiple comparisons, Figure 11b). Although there was no statistical difference between the final percentages of regenerated tissue between groups, ($p<0.05$, Kruskal-Wallis test with Dunn's multiple comparisons, **Figure 11B**), all coral nubbins in the 0 NTU control group had achieved 100% healing by 9 days post-wounding, while there was still incomplete healing in the turbidity-treated groups by14 days (**Figure 12**). The delay in wound healing from turbidity was consistent with our previous findings (May et al. 2023), which demonstrates reduced tissue regeneration of *O. faveolata* following a 96-h exposure to average peak turbidities of 4, 20, and 30 NTU. Although the wounds eventually healed while in a laboratory setting, it's important to consider that in the wild, the delay in healing would expose the corals with open wounds to additional pathogens or stressors, which may prevent complete wound healing from occurring.

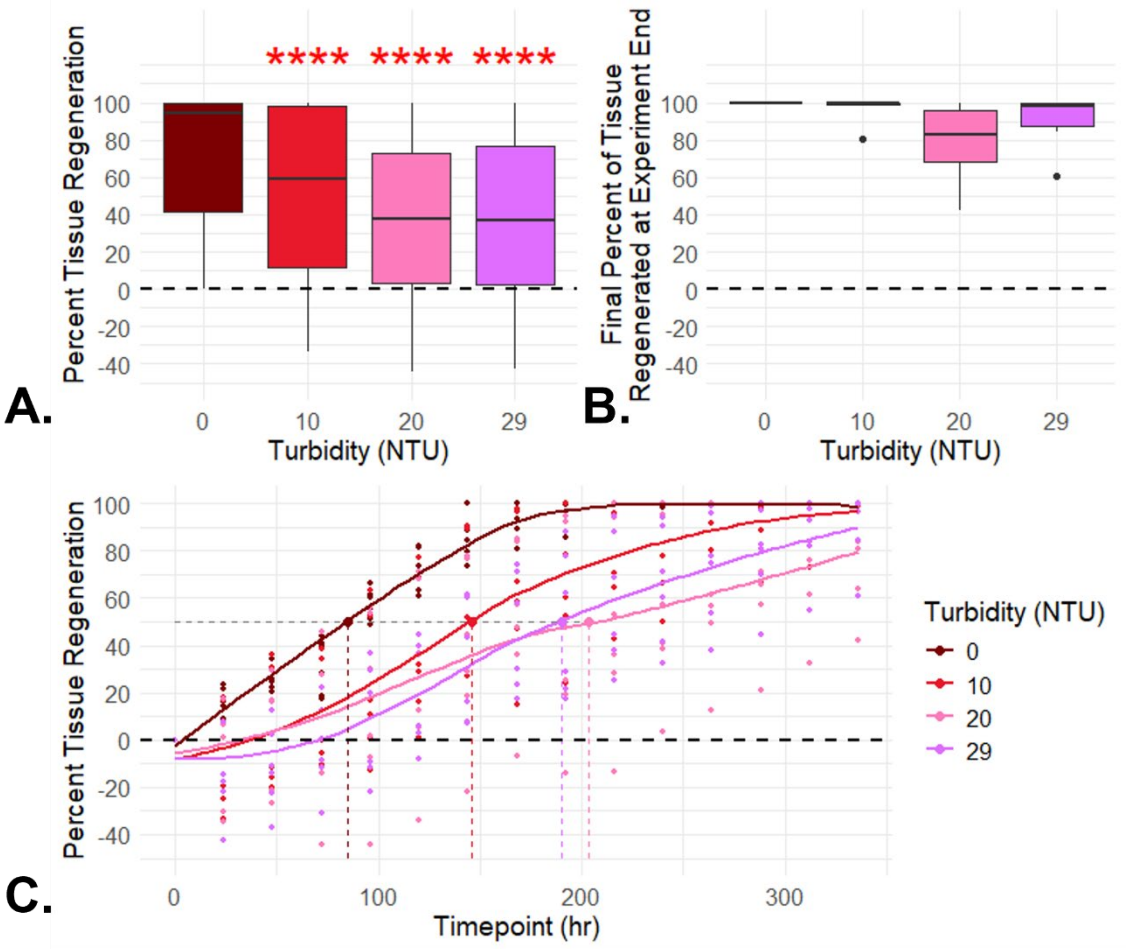

Figure 9. Wound healing capabilities (measured as percentage of tissue regeneration) of corals after a 90-day turbidity dose-response experiment. **A)** A box and whisker plot showing the repeated measures tissue regeneration data of each treatment over the 90-day experiment. The percentages of regenerated tissue in all tested turbidity treatments were significantly lower than those in the 0 NTU control group ($p=0.01$, $p<0.0001$, $p<0.0001$, respectively, pairwise comparisons using paired t-tests). **B)** Final percentages of regenerated tissue in each treatment after the 14-day healing period post-wounding. There was no significant difference in the final measure of tissue regeneration between any treatment groups ($p<0.05$, Kruskal-Wallis test with Dunn's multiple comparisons). However, all coral nubbins in the 0 NTU had regenerated 100% of their wounded tissue, while none of the tested turbidity treatments achieved 100% healing in all nubbin replicates by this time. **C)** Daily percentages of tissue regeneration in each treatment group over the 14-day healing period. A smooth curve fitted using LOESS (locally estimated scatterplot smoothing) is shown for each turbidity condition to highlight trends over time. Vertical dashed lines represent the points in the healing process in which the mean regenerated tissue was 50 % in all treatment groups, determined using calculated xmid values in a non-linear mixed effects model. This illustrates a delay in healing of 2.6 days in the 10 NTU group, 5 days in the 20 NTU group, and 4.4 days in the 29 NTU group compared with the 0 NTU control group.

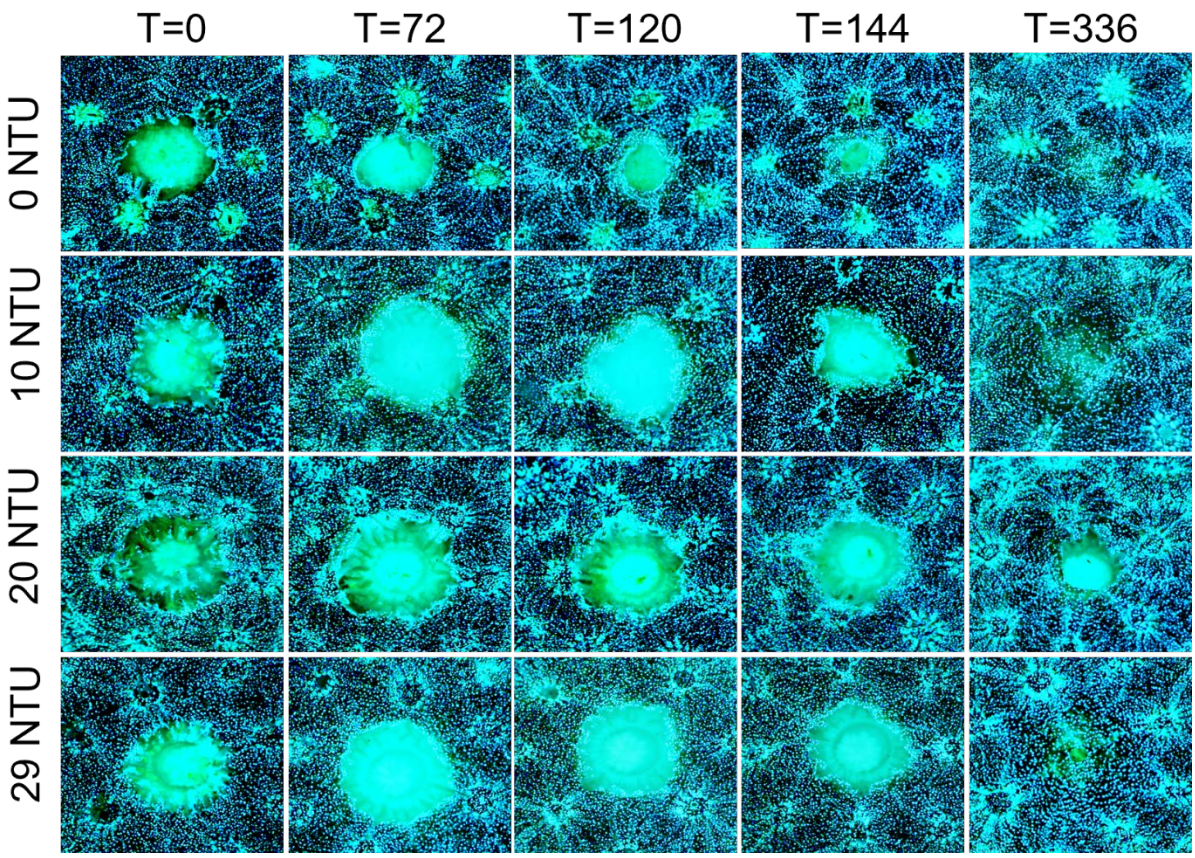

Figure 10. Fluorescent images displaying wounds of a single representative *O. faveolata* nubbins at 0, 72, 120, 144, and 336 h post wounding, and exposed to 0, 10, 20, and 29 NTU turbidity. Coral nubbins were lacerated at two weeks prior to experiment end and measured daily for 14 days.

3.2.6. Effect of turbidity on energy reserves of the *O. faveolata* holobiont

Total soluble proteins were significantly decreased in the 20 NTU treatment compared to the 0 NTU control group (p=0.0128, Kruskal-Wallis test with Dunn's multiple comparisons) (**Figure 13A**). Total soluble lipids were significantly decreased in the 10 NTU treatment compared to the 0 NTU control group (p=0.0076, Kruskal-Wallis test with Dunn's multiple comparisons) (**Figure 13B**).

The decrease in proteins and lipids was not unexpected with increased turbidity stress, if compensatory processes are unable to fully respond to a turbidity stress. However, these data present a conundrum as to why there is a significant effect for total soluble proteins at 20 NTU, but not at 10 or 29 NTU, similarly for the total lipids, there is a significant depletion in the lipid pool in fragments treated with 10 NTU but not at 20 or 29 NTU. If we focus on the trends in the data, we see that the 10 and 20 NTU are reduced compared to the control, while the 29 NTU is much less affected than the 10 or the 20 NTU treatments for both protein and lipids. A plausible explanation for the 10 and 20 NTU is that the statistical significance is sensitive to variation and in both cases the treatments with the smallest variation are those that are

significant although in absolute concentrations both show a depletion in their respective energy stores. A second consideration is to examine how these energy pools are replenished in this experimental set-up. Two primary sources of energy for these nubbins are the twice-weekly feeding of a complex diet and their photosynthetic efficiency. Over the course of the experiment, we observe from other endpoints that all of the treatments were keeping pace with the control in growth metrics, likely aided by the heterotopic feeding of a complex diet, and needing to recruit resources from the protein and lipid pools to accomplish this. Growth is not differentially affected across treatments; therefore, it is reasonable to speculate that the heterotrophic feeding could be balancing or replenishing the energy stores being used for growth so there is no net loss of the energy stores. Photosynthesis which contributes to energy stores, particularly to the lipid pool, shows compensatory mechanisms successfully being recruited to acclimate to the stress of increasing turbidity. The symbiotic algae at 29 NTU are able to significantly increase photosynthetic efficiency over the control after 90 days. The process of compensating for the turbidity stress at 10 and 20 NTU may be expending more energy than is being replenished, while the 29 NTU seems to provide a condition that allows photoacclimation to proceed more efficiently. It is important to recognize that the total protein and total lipid measurement were from fragments that had experienced a trauma from incurring a laceration two weeks before these measurements were collected. The trauma of the loss of tissue and some degree of skeleton from the laceration and then mounting a healing response while being exposed to varying turbid conditions, conceivably contributed to the profile of the protein and lipid pools observed at experiment end. The protein and lipid concentrations were one snapshot of a complex interplay between processes that are producing and storing energy (photosynthesis, heterotrophic feeding) contrasted against processes that are using energy resources to stabilize physiological systems against disturbances. This experiment included disturbances such as physical particles from turbidity shading, abrading and adhering to tissues as well as responding to a wound and regenerating tissue. It is possible that the results reflect a point in the overall dynamics of metabolism and the processes of anabolism and catabolism that may not provide a complete picture. If samples could be taken throughout the course of the experiment rather than just at the end, the processes in response to turbidity and wound healing could be more conclusive. While total protein and total lipid relative to organic fraction is informative for the overall energy state, in the future, looking at specific proteins or lipids could be more informative on how turbidity is impacting the corals on the molecular level and what type of protective mechanisms are at play. Finally, if heterotrophic feeding is significantly enhancing energy stores (and potentially masking the extent of possible effects), restricting the diet may provide more distinction in responses to turbidity levels among the assessment endpoints used in this study and better clarity for characterizing the effects of turbidity on coral health.

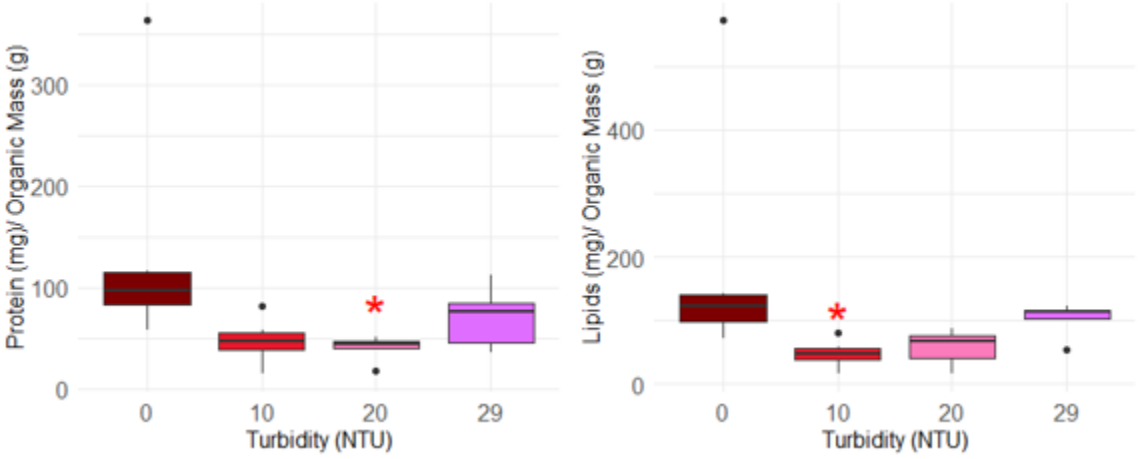

Figure 11. Total soluble proteins and lipids of *O. faveolata* after a 90-day turbidity dose-response experiment. **A)** Total soluble protein content (protein (mg)/organic mass (g)) measured at the experiment end. Total soluble protein was significantly decreased in the 20 NTU treatment compared with the 0 NTU control (p=0.0128, Kruskal-Wallis test with Dunn's multiple comparisons). **B)** Total soluble lipid content (lipids (mg)/organic mass (g)) measured at the experiment end. Lipid content was significantly decreased at 10 NTU compared to the 0 NTU control (p=0.0076, Kruskal-Wallis test with Dunn's multiple comparisons).

3.3. Dual stressor experiment: turbidity exposure with elevated temperature

3.3.1. Water quality

Temperature remained consistent within a range of 0.5 °C (27.6-28.1 °C) and 0.9 °C (29.1-30.0 °C) throughout the experiment for the 28 °C and 30 °C treatments, respectively (**Figure 14A**). Treatment beakers were kept in separate water baths for each temperature. This enabled better temperature control over the previous experiment (which was controlled by the air temperature in the environmental chamber), resulting in stable temperature measurements throughout this experiment.

The pH was consistent throughout the study, with 0 NTU treatments slightly higher than the treatment groups exposed to a target turbidity of 29 NTU (**Figure 14B**). For all treatments, pH ranged within 0.44 units (7.78-8.22). The pH increased slightly with fresh treatments immediately after renewal. The lowering of pH between treatment renewals is likely due to the accumulation of byproducts of cellular respiration (CO_2), mucus shedding and other metabolic by-products, which are removed when the treatments and beakers are changed.

Salinity was consistent throughout the experiment, with an average of 36.65 ppt and a range of 35.96-37.83 ppt for all treatments (**Figure 14C**). The highest salinity measurements collected were on April 16, 2024 (63 days into the experiment), before the treatment change for the 29 NTU at 30 °C treatment (mean = 37.67 ppt). It was discovered that the glass beaker lids were not fully covering the treatment beakers for all replicates in this treatment resulting in evaporation and an increase in salinity.

However, this change in salinity is considered minimal; therefore, it should have no impact on the experimental results.

Daily minimums for turbidity measurements were from the control temperature (28 °C). It was the lowest on April 8 and 9, 2024 (55 and 56 days into the experiment), with an average turbidity of 11.4 NTU and 10.0 NTU, respectively (**Figure 14D**). During this time period, there was an increase in sediment adherence to coral eggcrate louver stands and Teflon mounting pegs, and with sediment accumulation on top of the coral surface. In the turbidity treatment exposed to the elevated temperature (30 °C), the lowest daily minimum occurred on April 7, 2024 (day 54 of the experiment), where the average turbidity was 17.0 NTU. This decrease was consistent between all treatment groups. We believe these brief deviations in NTU did not affect the overall experiment based on no observable changes in maximum quantum yield or coral growth during this time period. The behavior of the turbidity seemed to be isolated to a particular treatment batch, even though there was only one sediment source. Aside from these specific timepoints, the daily resuspension of accumulated sediment on surfaces within treatment vessels allowed the target NTU of treatments to be consistently achieved within each respective treatment vessel throughout this study.

Overall, water quality measurements remained stable throughout the experiment with salinity and pH remaining consistent among all treatment groups. Temperature and turbidity maintained their targeted levels (**Table 6**).

Table 6. Descriptive statistics for water quality measurements collected throughout the 90-day dual stressor experiment with *Orbicella faveolata*.

	0 NTU 28 °C	**0 NTU 28 °C**	**29 NTU 28 °C**	**29 NTU 28 °C**	**0 NTU 30 °C**	**0 NTU 30 °C**	**29 NTU 30 °C**	**29 NTU 30 °C**
Parameter	Mean	SD	Mean	SD	Mean	SD	Mean	SD
Temperature (°C)	27.9161	0.0733	27.9423	0.0734	29.8676	0.0878	29.8784	0.0895
Salinity (ppt)	36.6836	0.2953	36.6129	0.2170	36.6042	0.2374	36.6413	0.2898
pH	7.9970	0.0711	7.9331	0.0653	8.0080	0.0753	7.9366	0.0593
Turbidity (NTU)	0.4346	0.1367	27.6886	4.3318	0.4318	0.1219	28.2485	3.9953

A.

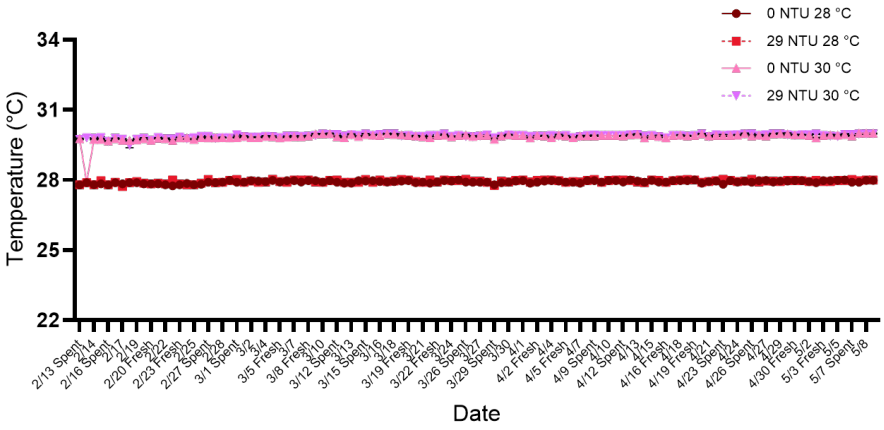
0 NTU 28 °C
29 NTU 28 °C
0 NTU 30 °C
29 NTU 30 °C
Temperature (°C)
Date

B.

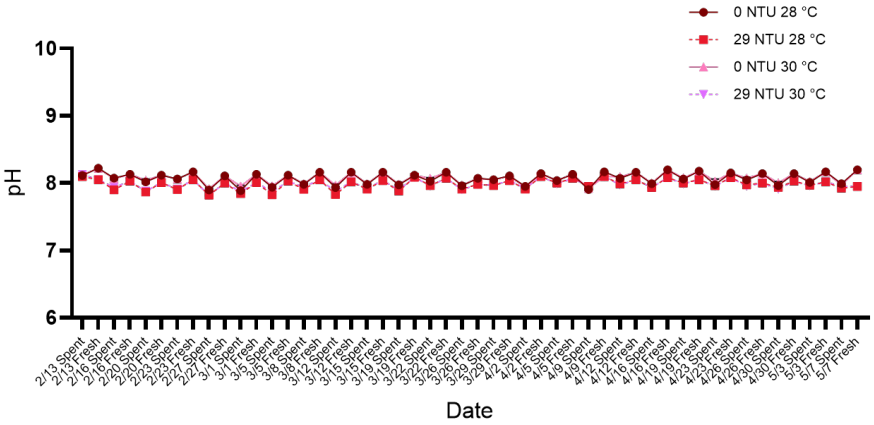
0 NTU 28 °C
29 NTU 28 °C
0 NTU 30 °C
29 NTU 30 °C
pH
Date

C.

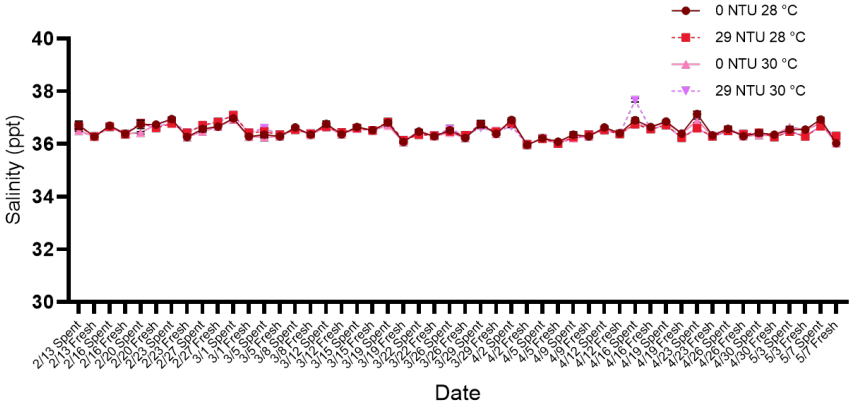
0 NTU 28 °C
29 NTU 28 °C
0 NTU 30 °C
29 NTU 30 °C
Salinity (ppt)
Date

D.

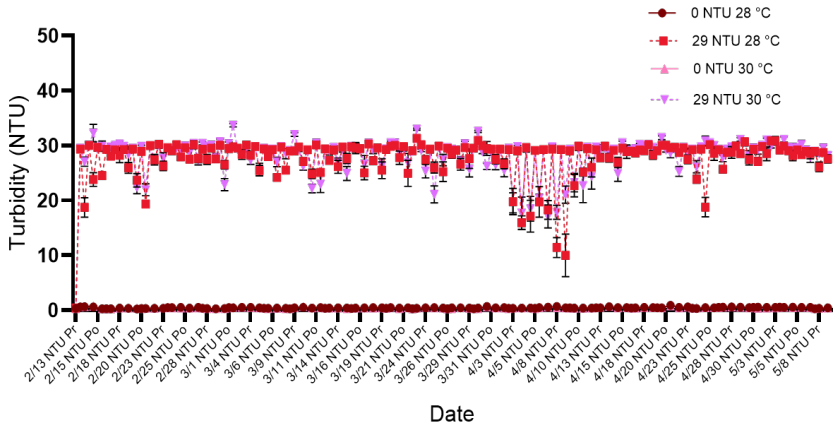
0 NTU 28 °C
29 NTU 28 °C
0 NTU 30 °C
29 NTU 30 °C
Turbidity (NTU)
Date

Figure 12. Water quality measurements collected throughout the 90-day dual stressor experiment (29 NTU and 30 °C) from "Fresh" and "Spent" treatments. **A)** Average temperature (°C) measured daily for each treatment; **B)** average pH measured twice per week from each treatment; **C)** average salinity (ppt) measured twice per week from each treatment; **D)** average turbidity (NTU) measured twice each day throughout the experiment. "Pr" and "Po" designations on each date indicate whether the parameter was measured before (pre) or after (post) the settled sediment was resuspended in each treatment vessel. Error bars represent standard error of the mean.

3.3.2. Effect of turbidity and elevated temperature on photosynthetic efficiency of *O. faveolata* algal symbionts

Both elevated temperature (30 °C) and turbidity (29 NTU) significantly reduced the photosynthetic efficiency of *O. faveolata* algal symbionts (measured as maximum quantum yield, Fv/Fm) over the 90-day dual stressor experiment ($p=0.000187$, 0.031405, respectively, two-way ANOVA) (**Figure 15A**). However, by the experiment end, symbionts appear to have photoacclimated, as there were no significant differences in Fv/Fm values between groups ($p>0.1$, two-way ANOVA, **Figure 15B**). Neither temperature nor turbidity had a significant effect on changes in Fv/Fm over time ($p>0.05$, linear mixed-effects model, **Figure 15c**) and there was no significant interaction between the two variables ($p=0.350354$, two-way ANOVA, **Figure 15D**). The maximum quantum yield of all test nubbins was within a normal range (~0.6) (**Figure 16**) and remained stable throughout the experiment with a fluctuation of ~0.03 for each treatment.

These results indicate that while both variables independently influence Fv/Fm, elevated temperatures do not exacerbate the effects of turbidity on the photosynthetic efficiency of in hospite algal symbionts (*Cladocopium* sp.) in *O. faveolata*. The data also demonstrate the dynamic profile of the algal symbionts undergoing photoacclimation. The mechanism by which this occurred was not determined in this study. There are several responses that can lead to photoacclimation that include increased algal symbiont cell density, increase in chlorophyll *a* content, and increases in the number and size of chloroplasts (Junjie et al. 2014). Our results only eliminate increased algal cell density as contributing to photoacclimation, as this was unchanged across treatments and was statistically confirmed through an ANCOVA with symbiont density as a covariate for changes in Fv/Fm ($p<0.05$).

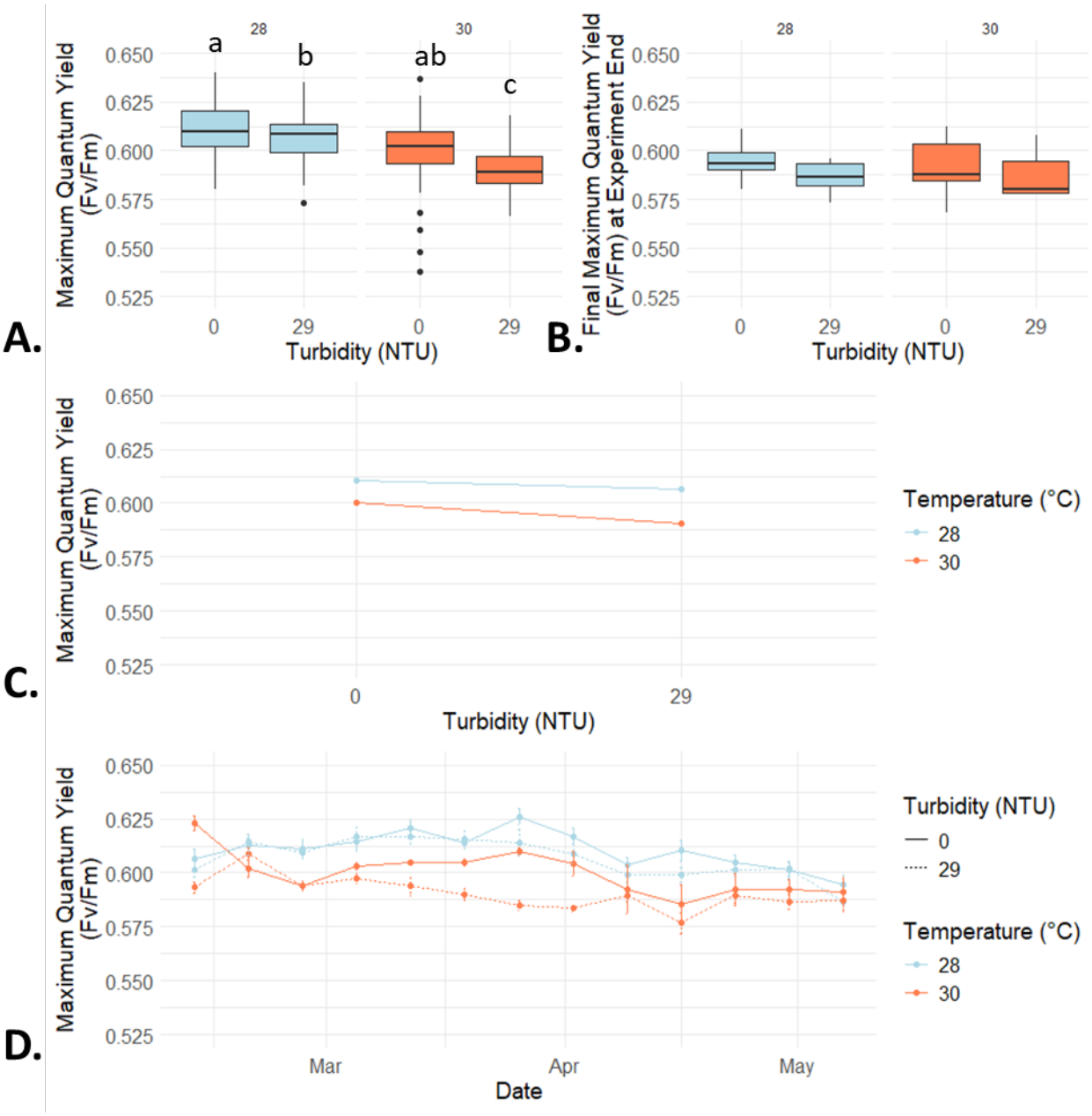

Figure 13. Maximum quantum yield (Fv/Fm) of *O. faveolata* nubbins in a 90-day dual-stressor experiment testing for effects of temperature (28°C, 30 °C) and turbidity (0 NTU, 29 NTU). **A)** A box and whisker plot showing the repeated measures Fv/Fm data of each treatment over the 90-day experiment. Both elevated temperature (30 °C) and turbidity (29 NTU) significantly reduced the Fv/Fm ($p = 0.000187$, 0.031405, respectively, two-way ANOVA). **B)** Final measurements of Fv/Fm of each treatment taken on the last day of the experiment. There was no significant difference in Fv/Fm across treatment groups (i.e., the maximum quantum yield did not differ from each other) ($p<0.05$, two-way ANOVA). **C)** Interaction plot showing the relationship between temperature and turbidity on Fv/Fm. There was no significant interaction between temperature and turbidity in regards to Fv/Fm ($p=0.350354$, two-way ANOVA). **D)** Weekly averages of maximum quantum yield (Fv/Fm) in

each treatment group over the course of the experiment. Weekly changes in Fv/Fm were not significantly influenced by either temperature or turbidity ($p>0.05$, linear mixed effects model).

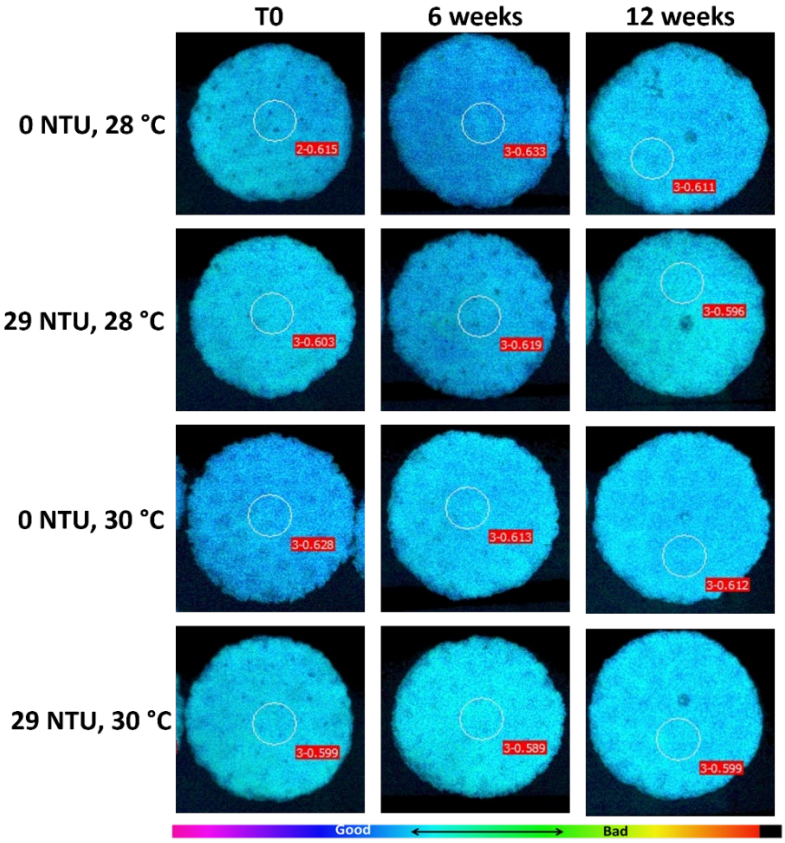

Figure 14. Representative pulse amplitude modulated fluorometry images of *Orbicella faveolata* fragments used to determine maximum quantum yield (Fv/Fm) in the dual stressor experiment. Chlorophyll *a* fluorescence images are of the same coral nubbin for each treatment over time. Images from week 12 show the healing wound used in the tissue regeneration assay (dark area in center of images). The white circles on each image represent the area of interest used to measure Fv/Fm (values in the red box on each image). A heat map below the image grouping shows the relative color with respect to chlorophyll *a* fluorescence, with blue colors indicating higher fluorescence and red indicating lower fluorescence indicative of the relative condition of the algal symbiont.

3.3.3. Effect of turbidity and elevated temperature on *O. faveolata* symbiont density

Neither turbidity (29 NTU) nor temperature (30 °C) had any effect on the average symbiont density (number of algal cells per µm² of gastrodermis) measured on the final day of the experiment ($p = 0.1808$, $p = 0.5176$, respectively, two-way ANOVA) (**Figure 17**). It is possible that this lack of an effect is driven by the large variation in

symbiont density between coral nubbins, as there is a trend in the plotted data that indicates an additive interaction between temperature and turbidity on reducing symbiont density (**Figure 17B**), though statistically this interaction is not significant (0.4099, two-way ANOVA).

Algal symbiont density can increase or decrease depending on the type and degree of stress placed on the symbiotic relationship. For example, in conditions that create oxidative stress, the algal symbiont may undergo symbiophagy (Downs et al. 2009) or the symbiont maybe expelled from its host through exocytosis (Steen & Muscatine 1987; Gates et al. 1992). Algal symbiont density can be ramped up as a compensatory mechanism from reduced light conditions (Jones et al. 2020), though in fact bleach if placed in darkness, depending on the duration. The fact that algal symbiont density did not change across treatments is an indication that the degree and duration of the dual temperature and turbidity exposures were not sufficient to modulate the symbiosis between the *O. faveolata* nubbins and algal cells. However, taking into consideration the plotted data, it suggests a reduction in algal cells in the 29 NTU and 30 °C (**Figure 17**), this would be consistent with the observed significant reduction in photosynthetic efficiency over time (**Figure 15 A & D**).

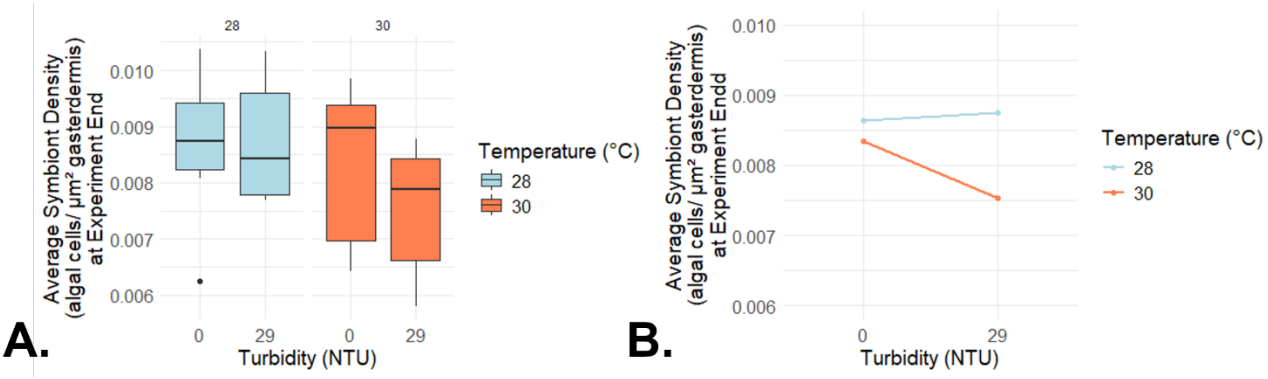

Figure 15. Average symbiont density (dinoflagellate cells per µm^2 of gastrodermal tissue) in corals at the end of a 90-day dual-stressor experiment testing for effects of temperature (28°C, 30 °C) and turbidity (0 NTU, 29 NTU). **A**) Box and whisker plot of algal symbiont density in *O. faveolata* gastrodermal tissues at the 90-day experiment end. There was no significant effect from temperature or turbidity on average symbiont density (p = 0.1808, p = 0.5176, respectively, two-way ANOVA). **B**) Interaction plot showing the relationship between temperature and turbidity on symbiont density. While there is an apparent trend showing an additive interaction between the two variables, this interaction was not statistically significant (0.4099, two-way ANOVA).

3.3.4. Effect of turbidity and elevated temperature on coral growth

Turbidity (29 NTU) had a significant negative effect on both *O. faveolata* growth (measured as the percent increase in calculated dry weight) after 90 days (p = 0.000135, two-way ANOVA, **Figure 18A**) and on growth rate over time (p = <0.0001, linear

mixed-effects model, **Figure 18D**). This negative effect on the rate of growth is exacerbated by elevated temperatures (30 °C) ($p<0.0001$, linear mixed-effects model, **Figure 18C**). Elevated temperature (30 °C) alone did not significantly impact growth ($p = 0.28676$, two-way ANOVA, **Figure 18B**) or growth rate ($p = 0.706$, linear mixed-effects model, **Figure 18D**) over the course of the experiment.

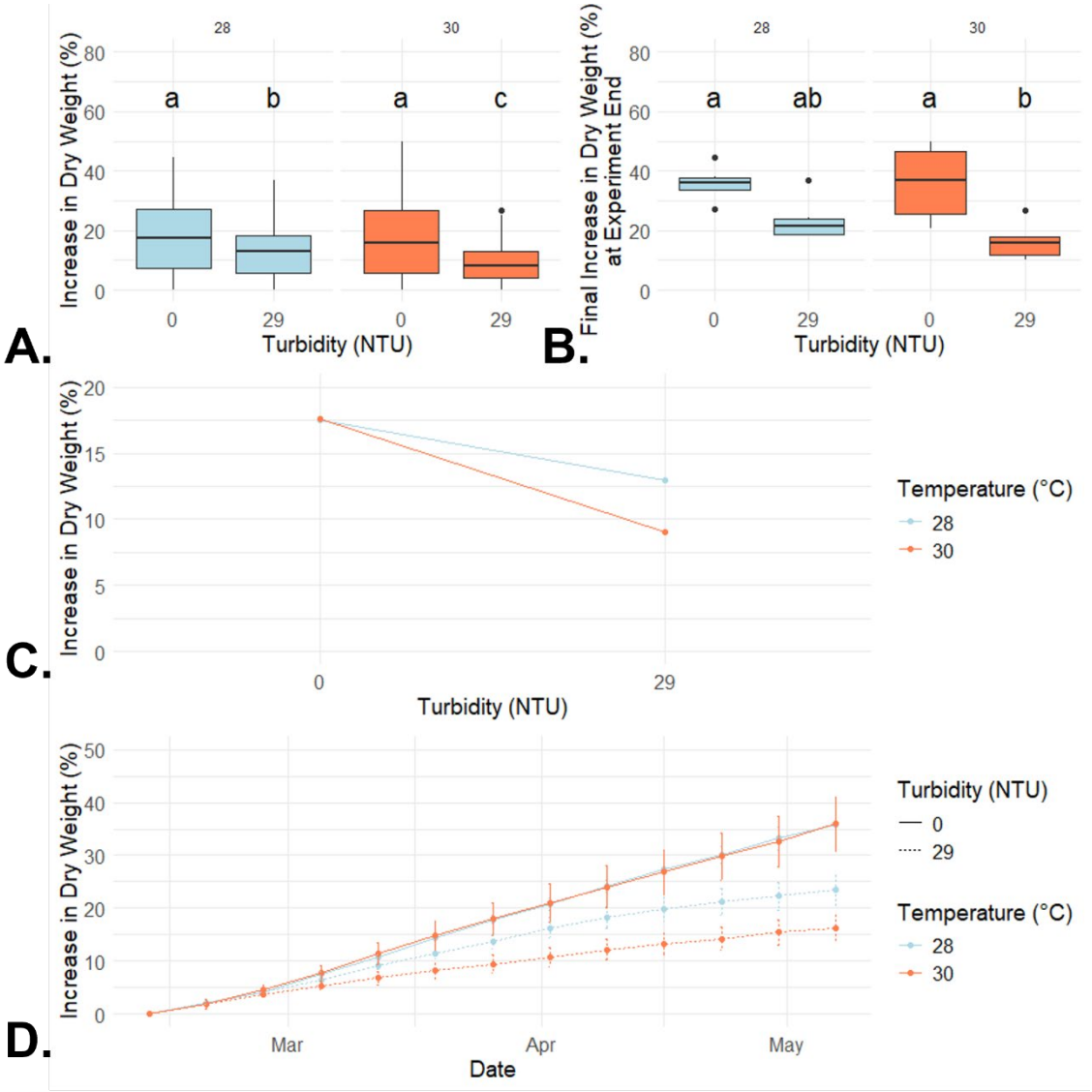

Figure 16. Changes in dry weight of *O. faveolata* nubbins in a 90-day dual-stressor experiment testing for effects of temperature (28 °C, 30 °C) and turbidity (0 NTU, 29 NTU). **A**) A box and whisker plot showing the repeated measures dry weight data of each treatment over the 90-day experiment. Turbidity alone (29 NTU) had a significant negative effect on coral growth ($p = 0.00135$, two-way ANOVA). **B**) Final measurements of each treatment taken on the last day of the experiment. Turbidity alone (29 NTU) had a significant negative effect on the total increase in dry weight ($p = 0.001346$, two-way ANOVA) **C**) Interaction plot showing the relationship between temperature and turbidity on coral growth. There was no significant interaction between temperature and turbidity in regards to coral growth ($p<0.0001$, linear mixed effects model) with the negative impact from turbidity becoming more extreme at elevated temperatures. **D**) Weekly averages of dry weight increase (%) in each treatment group

over the course of the experiment. Turbidity had a significant negative effect on the change in dry weight over time, with corals in the 29 NTU groups growing significantly slower than their 0 NTU counterparts in either temperature ($p<0.0001$, linear mixed effects model).

Although the growth profiles and growth rates varied over time and across treatments, by experiment end, the nubbins in the turbidity treatments had significantly retarded growth compared to the no-turbidity treatments, while temperature alone did not affect growth. The mechanism(s) driving these responses were not determined in this study (**Figures 18A**). However, two main stress-related factors for coral that have been associated with anthropogenically turbid conditions are related to photophysiological dysregulation and energetic loss from particle abrasions or deposition of sediment onto coral tissues (López-Londoñ et al. 2021). Assessment endpoints of both factors were depressed in this study and likely contributed to the observed retarded growth in turbid treatments. Since photosynthetic efficiency also was depressed over the course of the experiment (**Figure 15A**) (although recovered to normal levels by experiment end) (**Figure 15B**), this could have contributed to reduced energy supplies for growth. While not statistically significant, the total soluble protein content of the fragments in turbid conditions regardless of temperature showed a negative trend, which could limit the protein-associated resources (e.g., amino acids) for growth. Total lipid concentrations were increased by temperature, but not significantly affected by turbidity. However, a specific subclass of lipids, the triglycerides, were reduced by turbidity and temperature (**Figure 22**). Triglycerides are a primary energy source for cellular metabolism which is critical for growth and tissue repair. This assessment endpoint provides additional evidence that reduced energy pools are contributing to the growth retardation observed.

3.3.5. Effects of turbidity and elevated temperature on coral tissue regeneration

Fragments of *O. faveolata* exposed to turbidity (29 NTU) had a significantly lower percentage of regenerated tissue after wounding ($p<0.0001$, two-way ANOVA, **Figure 19A**) and a slower rate of tissue regeneration over the healing period ($p=0.000147$, linear mixed-effects model, **Figure 19D**). While the differences in wound healing between treatments groups appear to lessen as healing time progresses (**Figure 19D**), at the end of the 14-day healing period, the high temperature/high turbidity treatment (30 °C, 29 NTU) still had regenerated significantly less tissue than the low temperature/no turbidity treatment (28°C, 0 NTU) ($p = 0.006185$, Kruskal-Wallis test on aggregated data with Parris-Nemenyi post-hoc test for multiple comparisons, **Figure 19B**). Except for one nubbin, the other 11 *O. faveolata* nubbins exposed to 0 NTU turbidity (regardless of temperature) reached 100% tissue regeneration by experiment termination, whereas only one nubbin subjected to 29 NTU was able to fully heal by this time (**Figures 19 and 20**).While temperature alone had no effect on the percentage of tissue regenerated after the two-week healing period ($p = 0.151$, repeated measures ANOVA, **Figure 19A**), coral fragments in the 30 °C temperature treatments did regenerate tissue significantly faster than those in the 28 °C temperature treatments ($p=0.013259$, linear mixed-effects model, **Figure**

19D). There was no significant interaction between temperature and turbidity in regards to wound healing capabilities (p = 0.7783, two-way ANOVA, **Figure 19C**).

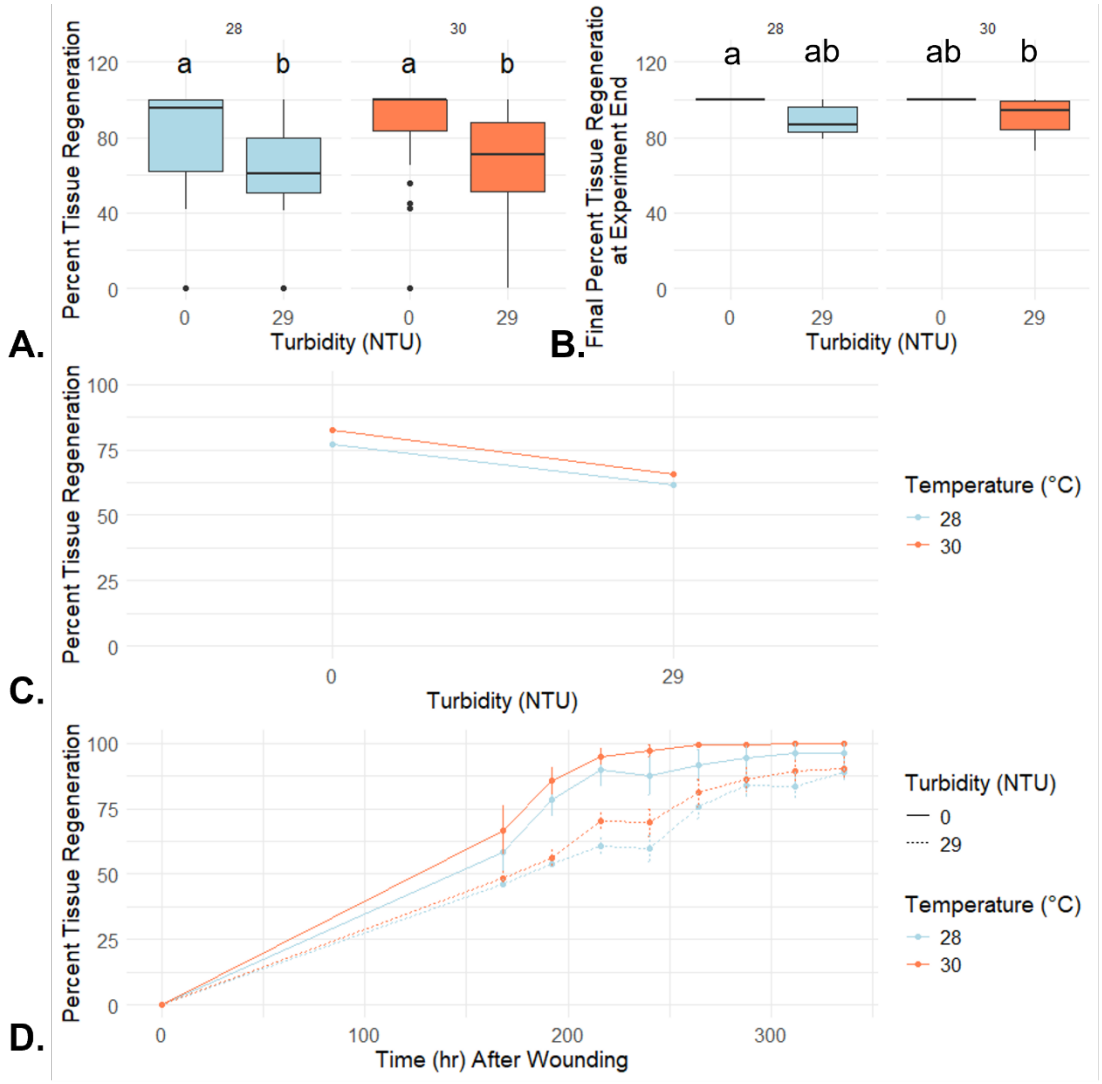

Figure 17. Changes tissue regeneration of wounded *O. faveolata* nubbins in a 90-day dual-stressor experiment testing for effects of temperature (28°C, 30 °C) and turbidity (0 NTU, 29 NTU). **A**) A box and whisker plot showing the repeated measures tissue regeneration (%) data of each treatment over the 90-day experiment. Fragments of *O. faveolata* exposed to turbidity (29 NTU) had a significantly lower percentage of regenerated tissue after wounding (p<0.0001, two-way ANOVA). **B**) Final percentages of regenerated tissue in each treatment on the last day of the experiment. The high temperature/high turbidity treatment (30°C, 29 NTU) had regenerated significantly less tissue than the low temperature/no turbidity treatment (28°C, 0 NTU) by the end of the 14-day healing period (p=0.006185, Kruskal-Wallis test on aggregated data with Parris-Nemenyi post-hoc test for multiple comparisons). **C**) Interaction plot showing the relationship between temperature and turbidity on wound healing. There was no significant interaction between temperature and turbidity in regards to percent of tissue regeneration

(p=0.856, repeated measures ANOVA). **D**) Daily averages of tissue regeneration (%) in each treatment group over the course of the experiment. Accurate daily traces were impossible to achieve for the first week of the tissue regeneration assay due to the presence of mesentery filaments obscuring the tissue margin around the wound, therefore these measurements were omitted during analyses. Corals exposed to elevated temperature healed significantly faster than those in the 28°C groups (p=0.013259, linear mixed-effects model).

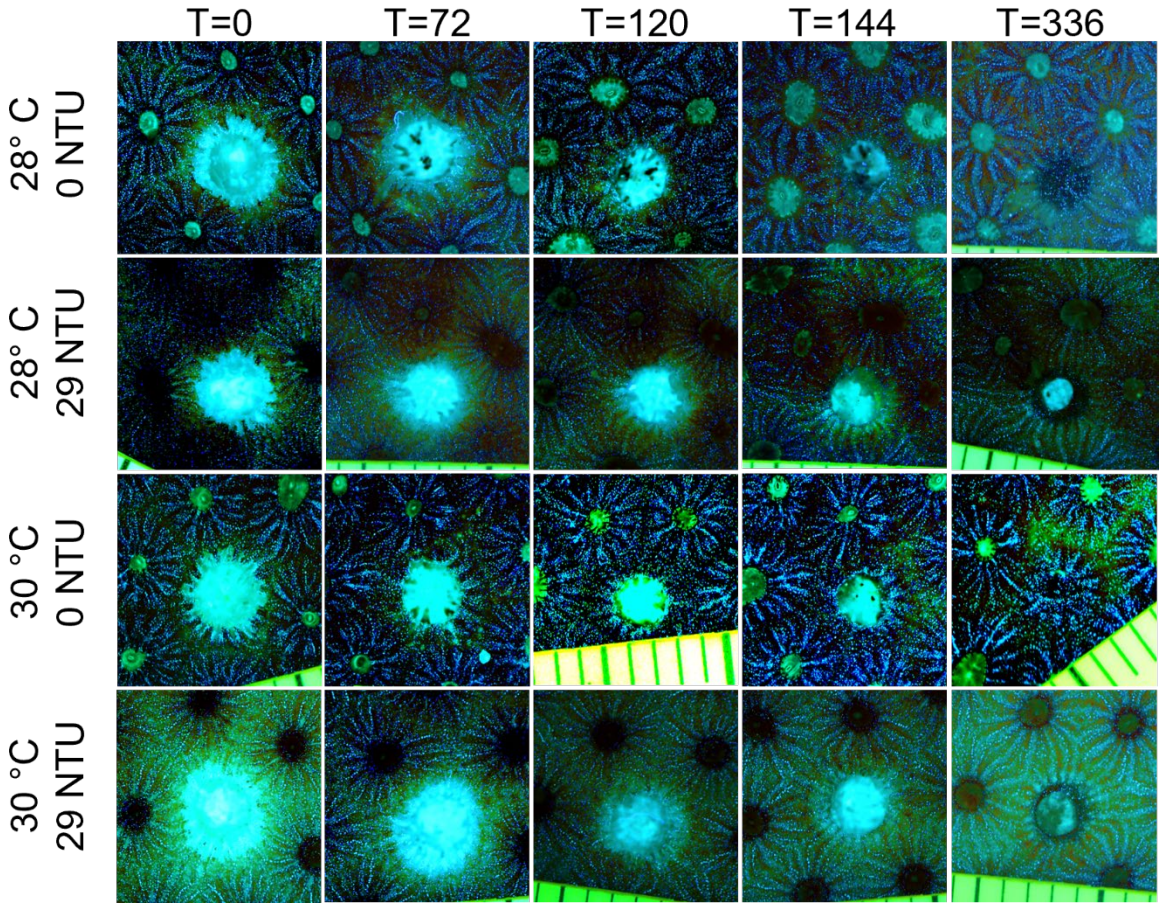

Figure 18. Fluorescent photomicrographs of *Orbicella faveolata* wounds in each dual stressor experiment treatment at 0, 72, 120, 144, and 336 h post wounding. Coral nubbins were lacerated two weeks prior to experiment end and tissue regeneration was measured daily. Although wounds started at approximately the same size, exposure to turbidity negatively affected wound healing ability.

3.3.6. Effect of turbidity and elevated temperature on energy reserves of the *O. faveolata* holobiont

Neither turbidity (29 NTU) nor temperature (30°C) had any effect on the concentration of soluble proteins (mg/g of organic mass) at experiment end (p=0.1929, p=0.7089, respectively, two-way ANOVA, **Figure 21 A, B**). Total lipid content of *O. faveolata* was significantly increased by elevated temperature (30 °C), which is observed when comparing the two turbidity controls (p = 0.0049, one-way ANOVA with Tukey's multiple comparisons) (**Figure 21B**). Although the 29 NTU

turbidity did not impact total lipids at the control temperature, there is a significant difference in lipid content when comparing the turbidity treatment and control at 30 °C ($p = 0.0115$, one-way ANOVA with Tukey's multiple comparisons). Thus, elevated temperature alone increased lipid content while turbidity at 29 NTU combined with the higher temperature did not change total lipids. While the main effects of turbidity (29 NTU) and temperature (30°C) on the concentration of soluble lipids (mg/g of organic mass) was not statistically significant ($p = 0.1875$, $p = 0.1027$, respectively, two-way ANOVA, **Figure 21C**), there was a significant antagonistic interaction between the two variables (0.0007364, two-way ANOVA, **Figure 21D**). This indicates that any increase in lipid concentration caused by turbidity (29 NTU) in a 28 °C environment is reversed in a 30 °C environment. When considering the maximum quantum yield response of the algal symbiont (**Figure 15A**), the 29 NTU/30°C treatment is significantly blunted during the course of the 90 days, which could help explain the reduction of total lipids in the same treatment. Meaning with the reduced photosynthetic efficiency of the algal symbionts over the course of the experiment, coupled with data showing these cells are not effectively undergoing photoacclimation to off-set the stressful conditions, can explain the reduced lipid concentrations.

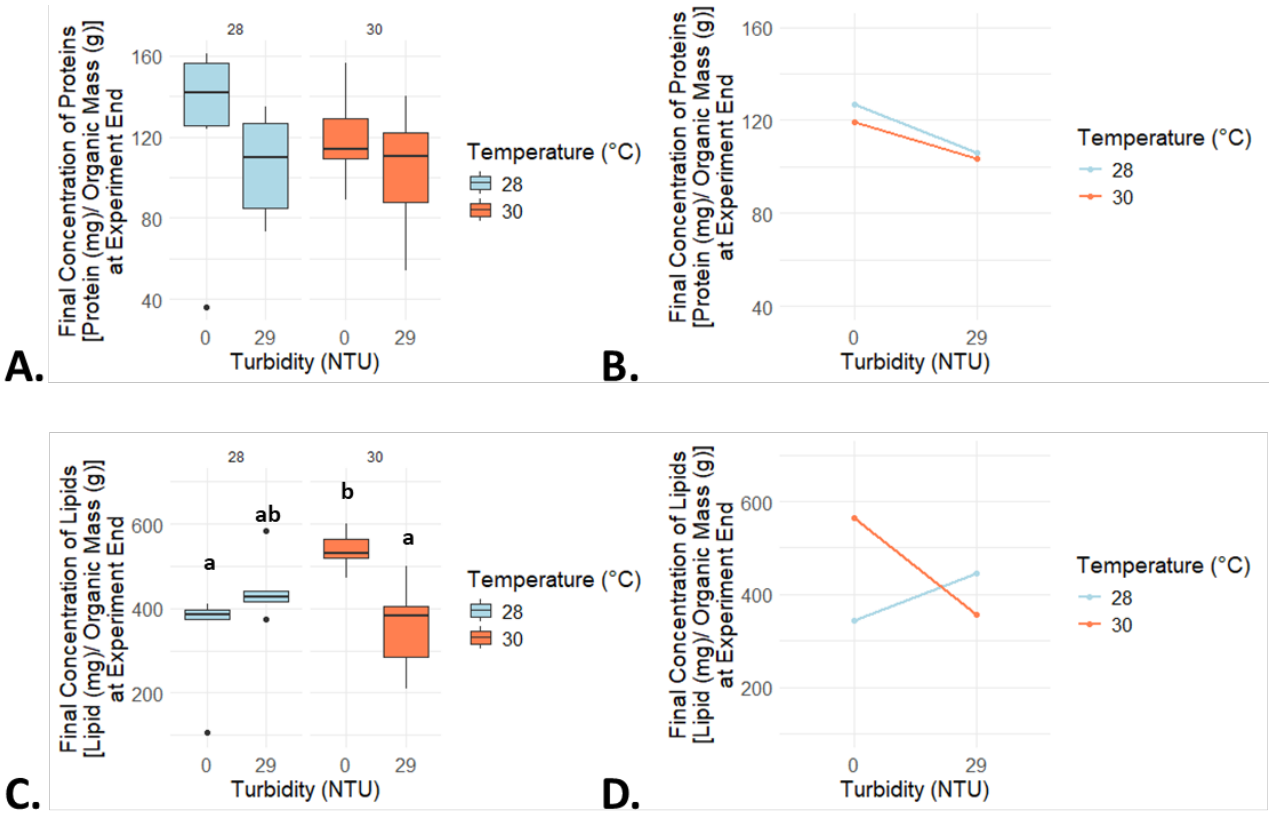

Figure 19. Changes in energy reserves (protein and lipid concentration) of *O. faveolata* nubbins in a 90-day dual-stressor experiment testing for effects of temperature (28°C, 30 °C) and turbidity (0 NTU, 29 NTU). **A)** Box and whisker plot of total soluble protein

concentration in the *Orbicella faveolata* holobiont at the experiment end. Neither turbidity (29 NTU) nor temperature (30°C) had any effect on the concentration of soluble proteins (mg/ g of organic mass) (p=0.1929, p=0.7089, respectively, two-way ANOVA). **B)** Interaction plot showing the relationship between temperature and turbidity on soluble protein concentration in exposed corals. There was no significant interaction between the variables in regards to protein concentration (p=0.8507, two-way ANOVA). **C)** Box and whisker plot of total soluble lipid concentration in the *Orbicella faveolata* holobiont at the experiment end. While the main effects of turbidity and temperature on lipid content were not significant (p=0.1875, p=0.1027, respectively, two-way ANOVA), the significantly higher concentration in the 30 °C control group compared to the 28 °C control group (p = 0.0115, one-way ANOVA with Tukey's multiple comparisons) and the lack of effect of temperature when turbidity is introduced (p>0.05, one-way ANOVA with Tukey's multiple comparisons) suggests that elevated temperature alone increased lipid content while turbidity at 29 NTU combined with the higher temperature did not change total lipids. **D)** Interaction plot showing the relationship between temperature and turbidity on soluble lipid concentration in exposed corals. There was a significant antagonistic interaction between the two variables (0.0007364, two-way ANOVA), indicating that any increase in lipid concentration caused by turbidity (29 NTU) in a 28°C environment is reversed in a 30°C environment.

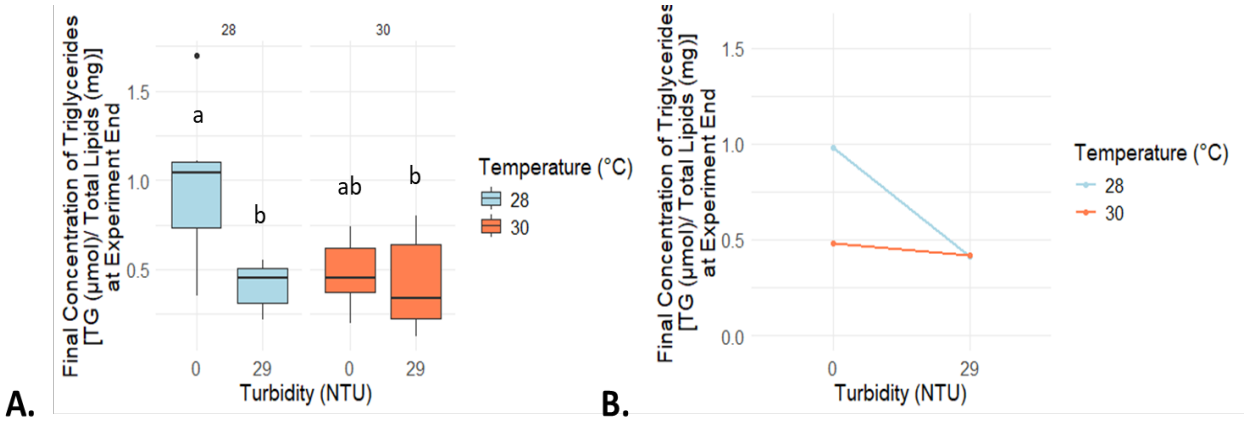

Figure 20. Changes in triglyceride content (µmol/mg of total lipids) of *O. faveolata* nubbins in a 90-day dual-stressor experiment testing for effects of temperature (28 °C, 30 °C) and turbidity (0 NTU, 29 NTU). **A**) Box and whisker plot of total triglyceride content in the *Orbicella faveolata* holobiont at the experiment end. Turbidity (29 NTU) has a significant negative impact on the concentration of triglycerides (p = 0.01584 two-way ANOVA). **B**) Interaction plot showing the relationship between temperature and turbidity on triglyceride content in exposed corals. There was no significant interaction between the variables in regards to triglyceride content (p=0.06218, two-way ANOVA), however, there is a substantially larger effect from turbidity at 28 °C compared to 30 °C.

Turbidity (29 NTU) had a significant negative impact on the concentration of triglycerides (µmol/mg of total lipids) measured at the experiment end (p = 0.01584,

repeated measures ANOVA (**Figure 22**). This appears to be driven by the significant reduction in triglycerides in 29 NTU groups in both temperatures (28 °C and 30 °C) ($p = 0.0234$, $p = 0.0406$, respectively, one-way ANOVA with Tukey's multiple comparisons test). Energy reserves in coral are formed through the transformation of excess carbon into triglycerides and wax esters. This result might indicate that with any stressors (temperature or turbidity), coral is using more energy than they are able to replenish in these large reserves (Piñón-González and Banaszak 2018). Examining specific lipid subclasses such as triglycerides (TG), provides a more specific assessment for how factors like turbidity or elevated temperature impact energy reserves that may be obscured by only evaluating the total lipid content.

In summary, this study has evaluated the effect(s) of chronic turbidity on the condition of *O. faveolata* from two perspectives, (1) different turbidity levels (dosage) and (2) a single turbidity level combined with an elevated temperature, that is below the bleaching threshold for this species. Both experiments used a combination of non-invasive and invasive assessment endpoints. Non-invasive endpoints were used to measure changes through time and cumulative effects at 90 days. For growth, the data provided a growth curve and growth rate over time, as well as the total growth for each treatment after 90 days. The photosynthetic performance of the algal symbionts also was assessed with weekly measurements of photosynthetic efficiency (Fv/Fm) over the course of the experiment. Although invasive, the ability of the fragments to recover from the trauma of an intentional laceration being exposed to turbidity or turbidity and elevated temperature for 10 weeks was also profiled over the last two weeks of both experiments. Lastly, terminal endpoints also were assessed, only capturing an ending snapshot of the cumulative impacts. These were measures of energy stores (total soluble proteins, total lipids and triglycerides, a subclass of energy-related lipids, measured only in the elevated temperature/turbidity experiment). Algal symbiont densities that can influence photosynthetic performance and nutrient supply for the coral host were measured from histological sections.

The first experiment asked: *Does turbidity level (dose) at or below the current water quality criterion under fixed conditions of duration and normal temperature, adversely affect O. faveolata?*

The data show that growth is not affected by turbidity levels of 0-29 NTU after 90 days at an optimal temperature (28 °C). Each of the turbidity levels seems to invoke processes that allow the algal symbionts to acclimate to the new conditions and compensate for the disturbance (i.e., turbidity) by increasing photosynthetic efficiency over time. This increase maybe considered an indication that a new energy-demand has been placed on the holobiont and photoacclimation is one mechanism algae use to off-set the energy expenditures from this response. Together these data indicate that the test organisms can respond and acclimate to all of the turbidity levels with no adverse effect after 90 days. This experiment cannot predict how long these corals can sustain this functional level, i.e., if the duration doubled would these fragments still be able to maintain growth performance and a higher level of photosynthetic efficiency. There is a hint in the biochemical data that suggests the energy reserves (protein and lipid) are potentially being depleted at a rate greater than they are being replenished, but not to the extent that physiological damage is indicated. One of the assessment endpoints that may

be of concern is the muting of the wound healing rate over the 90 days. Although ultimately most of the fragments healed, there were obvious differences in the time required for the wounds to heal in all of the turbidity treatments (10 NTU = 2.6-day delay, 20 NTU = 5-day delay and 29 NTU = 4.4-day delay). These delays represent a point of vulnerability for the coral as the prolonged exposure of open wounds provides additional time for opportunistic invasions (e.g., algae, microbes, pollutants) that otherwise would be protected with an intact tissue barrier.

The second experiment asked: *Does a two degree increase in temperature (above normal culture conditions) coupled with exposure to a fixed turbidity level of 29 NTU and duration, adversely affect O. faveolata?*

The data show that with elevated temperature and turbidity the trend in photosynthetic efficiency over the 90 days is depressed compared to 0 and 29 NTU conditions at 28°C. This indicates that the process of photoacclimation is being challenged when compared to the results in the first experiment that showed a robust ability for photoacclimation. By the end of 90 days, all treatments seemed to be converging to the same maximum quantum yield, albeit lower than the initial Fv/Fm. Although not significant (likely due to the variation between replicates), there is a trend showing a decrease in symbiotic algae density in samples exposed to turbidity (regardless of temperature) which supports the maximum quantum yield data of a depressed response to photoacclimation. Total growth and growth rate were both reduced with turbidity; increased temperature further retarded growth. Wound healing rate was reduced with turbidity exposure, though elevated temperature seemed to provide a degree of compensation by increasing growth rates in the 0 and 29 NTU treated fragments, compared to the 28°C treatments. Further, the amount of tissue regenerated under the high temperature/high turbidity treatment (30°C, 29 NTU) was significantly less than the low temperature/no turbidity treatment (28°C, 0 NTU) by the end of the 14-day healing period.

Each of these processes require energy to fuel the responses to new disturbances that challenge the plasticity boundaries of physiological responses (e.g., turbidity combined with small temperature increases). The ability to maintain energy reserves is one of the factors that determines the organism's phenotypic plasticity to accommodate an altered state to successfully respond to environmental stressors through acclimation or acclimatization. If the phenotypic (i.e., physiologic) plasticity of the organism is overwhelmed then impacts to fitness occur. Our data show that under the conditions and duration of this experiment *O. faveolata* fragments were able to maintain their soluble protein and total lipid pools. Interestingly, the elevated temperature without turbidity significantly increased the total lipid content. This positive response was ameliorated when both elevated temperature and turbidity were present, as the nubbins with combined stressors could only maintain lipid levels comparable to the 28 °C controls. However, when just the triglyceride subclass of lipid was measured, corals in either turbidity treatment showed significantly less triglyceride concentrations. Further, though not statistically significant, the no turbidity and elevated temperature also showed a trend toward a lower concentration. Together these data indicate there is a physiological and energetic cost to the *O. faveolata* nubbins with turbidity exposure that can be increased with elevated temperature. These corals are showing multiple signs of stress and

challenges to key processes such as growth and wound healing as well as declines in photosynthetic efficiency and triglyceride stores that function to support cellular metabolism. Our data seem to indicate that these *O. faveolata* fragments are at or near a threshold tipping point. Our assessment endpoints do not support the conclusion of no impact or that acclimation or acclimatization processes are robust against turbidity levels at the current Florida water quality criterion for turbidity when a small increase in temperature is added to this initial stressor. We are unable to predict whether with additional time under these conditions, the coral will return to their prior physiological state, acclimate to a new state, or continued exposure will prevent recovery once the stressors are removed.

4. CONCLUSIONS

Two challenge experiments were performed to examine the effects of chronic (90-day) turbidity exposure levels for determining turbidity water quality benchmarks that are protective of *Orbicella faveolata*. The first experiment focused on characterizing the dose-response of *O. faveolata* to various turbidity levels (10, 20, and 29 NTU) at 28 °C. The second experiment focused on determining how elevated temperature (30 °C) might influence the response of *O. faveolata* to turbidity at a level of 29 NTU. The endpoints evaluated for this report were growth, photosynthetic efficiency, energy reserves (total lipid and protein), wound healing, and symbiont density.

Water Quality

- Water quality measurements were consistent throughout the duration of the 90-day experiments. A consistent turbidity for all treatment groups in both experiments was maintained for the entire 90-day durations.

Photosynthetic Efficiency

- A significant increase in photosynthetic efficiency occurred in the dose-response experiment due to turbidity exposure (at 10, 20, and 29 NTU), which may be due to increased light diffusion (~5% decrease in PAR observed at 29 NTU in experimental conditions), and/or increased nutrient availability (e.g., organic matter associated with sediment, feeding regimen).
- Photosynthetic efficiency was significantly decreased due to 29 NTU turbidity and elevated temperature (30 °C) in the dual stressor experiment, indicating that photoacclimation processes of the algal symbiont were not effectively maintaining the maximum quantum yield over time. Although by the end of the experiment the algal photosynthetic activity was not significantly different across treatments over all Fv/Fm decreased compared to initial values.
- The contrasting result between experiments may be due to the morphology of *O. faveolata* nubbins used in the two experiments, as nubbins were more mounded in the dose-response experiment compared to the flatter nubbins used in the dual stressor experiment.

Symbiont Density

- Neither turbidity nor elevated temperature impacted symbiont density in either experiment. Thus, symbionts (*Cladocopium* sp.) within *O. faveolata* nubbins used in our exposure experiments seem to be resilient to turbidity

as high as 29 NTU and elevated temperature of 30 °C. Certain species of *Cladocopium* sp. have been found to be well-adapted to various hosts and habitats (e.g., light intensities) (LaJeunesse et al. 2018; Saad et al. 2022), thus changes in turbidity, and therefore light conditions, may not affect symbiont density significantly. It is important to note that while not statistically significant the symbiont density in the dual stressor experiment showed a negative trend.

Growth

- Growth was not affected by any level of turbidity in the dose-response experiment.
- Growth was decreased at 29 NTU at the elevated temperature of 30 °C in the dual-stressor experiment, indicating that temperature exacerbates negative effects of turbidity on *O. faveolata* growth.
- Exposure of *O. faveolata* nubbins to 29 NTU turbidity and elevated temperature (30 °C) may increase metabolic stress that results in reduced growth, as evidenced by the reduction in total lipids, triglyceride (TG) content, and photosynthetic yield.
- The reduction in maximum quantum yield of the algal symbionts in the 29 NTU, 30 °C treatment indicate a decline in primary energy production that can directly impacting lipid synthesis and energy storage, which further affected growth.

Wound Healing

- All levels of turbidity tested in the dose-response experiment (10, 20, and 29 NTU) reduced wound healing significantly throughout the two-week assay.
- Turbidity caused an evident delay in wound healing which we approximate to be 2.6 days in 10 NTU, 5 days in 20 NTU, and 4.4 days in 29 NTU. By 14 days post-wounding, any delay caused by turbidity is overcome, and the groups are able to regenerate a statistically similar percentage of tissue.
- Turbidity exposure of 29 NTU at 28 °C and 30 °C decreased tissue healing significantly throughout the two-week assay during the dual stressor experiment.
- Nubbins at 30 °C (regardless of turbidity exposure) healed significantly faster compared to the 28 °C treatments during the dual stressor experiment.
- Our results indicate independent effects of turbidity and temperature on the wound healing ability of *O. faveolata* nubbins.

- A decreased healing rate and delay to healing represent a point of vulnerability for the coral as the prolonged exposure of open wounds provides additional time for opportunistic invasions (e.g., algae, microbes, pollutants) that otherwise would be protected with an intact tissue barrier.

Energy Reserves

- Lower turbidity concentrations (10 NTU and 20 NTU) significantly decreased energy storage molecules (total lipids and total soluble proteins) by the end of the dose-response experiment, however lipids and proteins were not significantly impacted by 29 NTU turbidity exposure.
- Although no significant impacts were observed regarding total soluble proteins, total lipids were significantly increased in the 0 NTU, 30 °C treatment compared to the 0 NTU, 28 °C treatment and the 29 NTU, 30 °C treatment. This may indicate that at higher temperature certain lipid classes are upregulated.
- Examining specific lipid subclasses such as triglycerides (TG), provides a deeper understanding for how factors like turbidity or elevated temperature impact energy reserves. A turbidity of 29 NTU at both temperatures (28 °C and 30 °C) significantly decreased the concentration of TG in *O. faveolata* nubbins following the dual stressor experiment.
- Further studies to evaluate additional lipid subclasses could provide clearer insights into our results.
- Collecting samples during the wound healing process or along a time series during the turbidity exposures likely would provide clearer insights and better interpretation of the overall impacts to metabolism, performance and performance profiles of each bioindicator when exposed to environmental stressors such as turbidity and temperature.

5. REFERENCES

Anschutz, P., & Charbonnier, C. (2021). Sampling pore water at a centimeter resolution in sandy permeable sediments of lakes, streams, and coastal zones. *Limnology and Oceanography: Methods*, 19(2), pp.96-114. https://doi.org/10.1002/lom3.10408

Anthony, K. R. N., & Fabricius, K. E. (2000). Shifting roles of heterotrophy and autotrophy in coral energetics under varying turbidity. 252: 221-253. https://doi.org/10.1016/s0022-0981(00)00237-9

Ashey, J., McKelvie, H., Freeman, J., Shpilker, P., Zane, L. H., Becker, D. M., Cowen, L., Richmond, R. H., Paul, V. J., Seneca, F. O., & Putnam, H. M. (2024). Characterizing transcriptomic responses to sediment stress across location and morphology in reef-building corals. *PeerJ*, 12, p.e16654. https://doi.org/10.7717/peerj.16654

Bialek, E. L. (1966). Handbook of Oceanographic Tables. U.S. Naval Oceanographic Office, Washington, D.C. Available from: https://apps.dtic.mil/sti/pdfs/AD0655638.pdf

Bruckner, A.W. (2012). Factors contributing to the regional decline of *Montastraea annularis* (complex). Proceedings of the 12th International Coral Reef Symposium, Cairns, Australia, July 9-13. https://www.ncei.noaa.gov/data/oceans/coris/library/NOAA/CRCP/project/1028/Bruckner_2012_ICRS_decline_of_Montastrea.pdf [accessed 6-10-24].

Burgess, D. J., Duffy, E., Etzler, F., & Hickey, A. J. (2004). Particle Size Analysis: AAPS Workshop Report, Cosponsored by the Food and Drug Administration and the United States Pharmacopeia. *AAPS Journal,* 6: 23-34. https://doi.org/10.1208/aapsj060320

Coman, C., Solari, F. A., Hentschel, A., Sickmann, A., Zahedi, R. P., & Ahrends, R. (2016). Simultaneous Metabolite, Protein, Lipid Extraction (SIMPLEX): A combinatorial multimolecular omics approach for systems biology. *Mol. Cell. Proteomics*, 15: 1453-66. doi: 10.1074/mcp.M115.053702.

Dodge, R. E., & Vaisnys, J. R. (1977). Coral populations and growth patterns: responses to sedimentation and turbidity associated with dredging. *Journal of Marine Research*, 35: 715–730.

Dodge, R. E., Wyers, S. C., Frith, H. R., Knap, A. H., Smith, S. R., Cook, C. B., et al. (1984). Coral calcification rates by the buoyant weight technique: Effects of alizarin staining. *J. Exp. Mar. Biol. Ecol.,* 75: 217-232. https://doi.org/10.1016/0022-0981(84)90167-9

Downs, C. A., Kramarsky-Winter, E., Martinez, J., Kushmaro, A., Woodley, C. M., Loya, Y., Ostrander, G. K. (2009). Symbiophagy as a cellular mechanism for coral bleaching. *Autophagy*.5(2):211-6. https://doi.org/10.4161/auto.5.2.7405

Enochs, I. C., Manzello, D. P., Jones, P. R., Stamates, S. J., & Carsey, T. P. (2019). Seasonal carbonate chemistry dynamics on southeast Florida coral reefs: Localized acidification hotspots from navigational inlets. *Frontiers in Marine Science*, 6: 160. https://doi.org/10.3389/fmars.2019.00160

Erftemeijer, P. L., Riegl, B., Hoeksema, B. W., & Todd, P. A. (2012). Environmental impacts of dredging and other sediment disturbances on corals: a review. *Marine Pollution Bulletin*. 64(9): 1737-1765. https://doi.org/10.1016/j.marpolbul.2012.05.008

Federal Register. (2006). "Endangered and Threatened Wildlife and Plants; Adding Four Marine Taxa to the List of Threatened and Endangered Wildlife." 72 FR 16284. https://www.federalregister.gov/documents/2007/04/04/E7-6188/endangered-and-threatened-wildlife-and-plants-adding-four-marine-taxa-to-the-list-of-endangered-and-threatened-wildlife [Accessed 6/8/2024].

Federal Register. (2014). "Endangered and Threatened Wildlife and Plants: Final Listing Determinations on Proposal To List 66 Reef-Building Coral Species and To Reclassify Elkhorn and Staghorn Corals." 79 FR 53851. https://www.federalregister.gov/documents/2014/09/10/2014-20814/endangered-and-threatened-wildlife-and-plants-final-listing-determinations-on-proposal-to-list-66 [Accessed 6/8/2024].

Federal Register. (2023). "Endangered and Threatened Species; Critical Habitat for the Threatened Caribbean Corals. Federal Register." 88 FR 54026. Pp. 54026-54083. https://www.federalregister.gov/documents/2023/08/09/2023-16556/endangered-and-threatened-species-critical-habitat-for-the-threatened-caribbean-corals [Accessed 6/10/24].

Florida Administrative Code. (2016). F.A.C. 62-302.530 Table: Surface Water Quality Criteria http://www.flrules.org/gateway/ruleno.asp?id=62-302.530&Section=0 [Accessed 6/8/24].

Florida Department of Environmental Protection. (2023). 'DEP SOPs', Florida Department of Environmental Protection, 21 June, https://floridadep.gov/dear/quality-assurance/content/dep-sops [Accessed 6/15/24].

Gates, R.D., Baghdasarian, G. and Muscatine L. (1992). Temperature stress causes host cell detachment in symbiotic cnidarians: implications for coral bleaching. Biological Bulletin. 182:324-32.

Hennige, S. J., Smith, D. J., Perkins, R., Consalvey, M., Paterson, D. M., & Suggett, D. J. (2008). Photoacclimation, growth and distribution of massive coral species in clear and turbid waters. *Marine Ecology Progress Series.* 369: 77-88. https://doi.org/10.3354/meps07612

Jokiel, P. L., Maragos, J. E., & Franzisket, L. (1978). Coral growth: buoyant weight technique. In: Stoddart DR, Johannes RE, editors. Coral Reefs: Research Methods. Paris: UNESCO. 529–541.

Jones, R., Bessell-Browne, P., Fisher, R., Klonowski, W., & Slivkoff, M. (2016). Assessing the impacts of sediments from dredging on corals. *Marine Pollution Bulletin*. 102: 9-29. http://dx.doi.org/10.1016/j.marpolbul.2015.10.049

Jones, R., Giofre, N., Luter, H. M., Neoh, T. L., Fisher, R., & Duckworth, A. (2020). Responses of corals to chronic turbidity. *Scientific Reports*, 10: 4762. https://doi.org/10.1038/s41598-020-61712-w

Junjie, R.K., Browne, N.K., Erftemeijer, P.L.A., Todd, P.A. (2014) Impacts of sediments on coral energetics: partitioning the effects of turbidity and settling particles. PLoS ONE 9(9): e107195. doi:10.1371/journal.pone.0107195

Kitchener, B. G. B., Wainwrite, J., & Parsons, A. J. (2017). A review of the principles of turbidity measurement. *Progress in Physical Geography*. 41(5): 620-642. https://doi.org/10.1177/0309133317726540

LaJeunesse, T. C., Parkinson, J. E., Gabrielson, P. W., Jeong, H. J., Reimer, J. D., Voolstra, C. R., & Santos, S. R. (2018). Systematic revision of Symbiodiniaceae highlights the antiquity and diversity of coral endosymbionts. *Current Biology*, 28: 2570-2580. https://doi.org/10.1016/j.cub.2018.07.008

Larsen, T. C., Browne, N. K., Erichsen, A. C., Tun, K., & Todd, P. A. (2017). Modelling for management: Coral photo-physiology and growth potential under varying turbidity regimes. Ecological Modelling. 362: 1-12. http://dx.doi.org/10.1016/j.ecolmodel.2017.08.018

López-Londoño, T., Galindo-Martínez, C.T., Gómez-Campo, K. et al. (2021) Physiological and ecological consequences of the water optical properties degradation on reef corals. Coral Reefs 40:1243–1256. https://doi.org/10.1007/s00338-021-02133-7

Macdonald, R. K., Ridd, P. V., Whinney, J. C., Larcombe, P., & Neil, D. T. (2013). Towards environmental management of water turbidity within open coastal waters of the Great Barrier Reef. *Marine Pollution Bulletin*. 74: 82-94. https://doi.org/10.1016/j.marenvres.2022.105807

May, L. A., Burnett, A. R., Miller, C. V., Pisarski, E., Webster, L. F., Moffitt, Z. J., et al. (2020). Effect of Louisiana sweet crude oil on a Pacific coral, *Pocillopora damicornis*. *Aquat. Tox.,* 222: 105454. https://doi.org/10.1016/j.aquatox.2020.105454

May, L. A., Miller, C. V., Moffitt, Z. J., Balthis L., Karazsia, J., Wilber, P., et al. (2023). Acute turbidity exposures with Port of Miami sediments inhibit *Orbicella faveolata* tissue regeneration. *Mar. Pollut. Bull.,* 193: 115217. https://doi.org/10.1016/j.marpolbul.2023.115217

Miner, J. G., & Stein, R. A. (1996). Detection of predators and habitat choice by small bluegills: effects of turbidity and alternative prey. *Transactions of the American Fisheries Society*, 125: 97-103. https://doi.org/10.1577/1548-8659(1996)125<0097:dopahc>2.3.co;2

NMFS (2024). Mountainous Star Coral. https://www.fisheries.noaa.gov/species/mountainous-star-coral/overview [Accessed 6/10/24].

Piñón-González, V. M., & Banaszak, A. T. (2018). Effects of partial mortality on growth, reproduction and total lipid content in the Elkhorn coral *Acropora palmata*. *Frontiers in Marine Science*, 5: 396. https://doi.org/10.3389/fmars.2018.00396

Ralph, P. J., Schreiber, U., Gademann, R., Kühl, M., & Larkum, A. W. (2005). Coral photobiology studied with a new imaging pulse amplitude modulated fluorometer 1. Journal of Phycology, 41: 335-342. https://doi.org/10.1111/j.1529-8817.2005.04034.x

Saad, O. S., Lin, X., Ng, T. Y., Li, L., Ang, P., & Lin, S. (2022). Species richness and generalists–specialists mosaicism of symbiodiniacean symbionts in corals from Hong Kong revealed by high-throughput ITS sequencing. *Coral Reefs*, 41: 1-12. https://doi.org/10.1007/s00338-021-02196-6

Santana, E. F., Mies, M., Longo, G. O., Menezes, R., Aued, A. W., Luza, A. L., Bender, M. G., Segal, B., Floeter, S. R., & Francini-Filho, R. B. (2023). Turbidity shapes shallow Southwestern Atlantic benthic reef communities. *Marine Environmental Research*, 183: 105807. https://doi.org/10.1016/j.marenvres.2022.105807

Schneider, C. A., Rasband, W. S., & Eliceiri, K. W. (2012). NIH Image to ImageJ: 25 years of image analysis. *Nature Methods*. 9: 671–675. https://doi.org/10.1038/nmeth.2089

Sheridan, C., Grosjean, P., Leblud, J., Palmer, C. V., Kushmaro, A., & Eeckhaut, I. (2014). Sedimentation rapidly induces an immune response and depletes energy stores in a hard coral. *Coral reefs*, 33: 1067-1076. https://doi.org/10.1007/s00338-014-1202-x

Stafford-Smith, M. G. (1993). Sediment-rejection efficiency of 22 species of Australian scleractinian corals. *Marine Biology*. 115: 229-243. https://doi.org/10.1007/BF00346340

Stauber, J. L., Chariton, A., & Apte, S. (2016). Global change. In: Marine Ecotoxicology (pp. 273-313). Academic Press. https://doi.org/10.1016/b978-0-12-803371-5.00010-2

Steen, R.G. and Muscatine, L. (1987). Low temperature evokes rapid exocytosis of symbiotic algae by a sea anemone. *Biological Bulletin*. 172: 246-63.

Tuttle, L. J., & Donahue, M. J. (2022). Effects of sediment exposure on corals: a systematic review of experimental studies. *Environmental Evidence*, 11: 4. https://doi.org/10.1186/s13750-022-00256-0

US Environmental Protection Agency (1980) Manual of Analytical Methods for the Analysis of Pesticides in Humans and Environmental Samples. EPA-600/8-80-038. Research Triangle Park, NC. Pp.1-8. https://nepis.epa.gov/Exe/ZyNET.exe/20007QPD.TXT?ZyActionD=ZyDocument&Client=EPA&Index=1976+Thru+1980&Docs=&Query=&Time=&EndTime=&SearchMethod=1&TocRestrict=n&Toc=&TocEntry=&QField=&QFieldYear=&QFieldMonth=&QFieldDay=&IntQFieldOp=0&ExtQFieldOp=0&XmlQuery=&File=D%3A%5Czyfiles%5CIndex%20Data%5C76thru80%5CTxt%5C00000002%5C20007QPD.txt&User=ANONYMOUS&Password=anonymous&SortMethod=h%7C-&MaximumDocuments=1&FuzzyDegree=0&ImageQuality=r75g8/r75g8/x150y150g16/i425&Display=hpfr&DefSeekPage=x&SearchBack=ZyActionL&Back=ZyActionS&BackDesc=Results%20page&MaximumPages=1&ZyEntry=1&SeekPage=x&ZyPURL [Accessed 6/28/24].

US Environmental Protection Agency (1988). Water Quality Standards Criteria Summaries: A Compilation of State/Federal Criteria. Office of Water Regulations and Standard. EPA 440/5-88013. National Technical Information Service document #PB, Washington, D.C., pp. 89–141451. https://nepis.epa.gov/Exe/ZyNET.exe/00001NCW.TXT?ZyActionD=ZyDocument&Client=EPA&Index=1986+Thru+1990&Docs=&Query=&Time=&EndTime=&SearchMethod=1&TocRestrict=n&Toc=&TocEntry=&QField=&QFieldYear=&QFieldMonth=&QFieldDay=&IntQFieldOp=0&ExtQFieldOp=0&XmlQuery=&File=D%3A%5Czyfiles%5CIndex%20Data%5C86thru90%5CTxt%5C00000001%5C00001NCW.txt&User=ANONYMOUS&Password=anonymous&SortMethod=h%7C-MaximumDocuments=1&FuzzyDegree=0&ImageQuality=r75g8/r75g8/x150y150g16/i425&Display=hpfr&DefSeekPage=x&SearchBack=ZyActionL&Back=ZyActionS&BackDesc=Results%20page&MaximumPages=1&ZyEntry=1&SeekPage=x&ZyPURL [Accessed 6/8/24].

Wahab, M. A. A., Fromont, J., Gomez, O., Fisher, R., & Jones, R. (2017). Comparisons of benthic filter feeder communities before and after a large-scale capital dredging program. *Marine Pollution Bulletin,* 122: 176-193. https://doi.org/10.1016/j.marpolbul.2017.06.041

Wang, P., & Beck, T. M. (2017). Determining dredge-induced turbidity and sediment plume settling within an intracoastal waterway system. *Journal of Coastal Research*, 33: 243-253. https://doi.org/10.2112/jcoastres-d-16-00083.1

Wentworth, C.K., 1922. A scale of grade and class terms for clastic sediments. *The journal of geology*, 30(5), pp.377-392. https://doi.org/10.1086/622910

Whitall, D., Bricker, S., Cox, D., Baez, J., Stamates, J., Gregg, K., & Pagan, F. (2019). Southeast Florida Reef Tract Water Quality Assessment. In: NOAA Technical Memorandum NOS NCCOS 271. Silver Spring. https://doi.org/10.25923/kyft-ja41 (116 pages).

Zweifler (Zvifler), A., O'Leary, M., Morgan, K., Browne, N. K. (2021). Turbid Coral Reefs: Past, Present and Future—A Review. *Diversity.* 13, 251. https://doi.org/10.3390/d13060251

6. APPENDICES

6.1. Appendix A. Directory of Google Drive Links for Raw Data

Documents and Folders	Google Drive Links
Master Google Drive folder	• FL DEP Turbidity 2023-2024
Data documentation: experiment 1	• Experiment 1: Data documentation
Data documentation: experiment 2	• Experiment 2: Data documentation
Lab notebook (experiment details) entries: experiment 1	• Experiment 1: Lab notebook - Google Drive
Lab notebook (experiment details) entries: experiment 2	• Experiment 2: Lab notebook – Google Drive

6.2. Appendix B. Google Drive Links to Raw Data Sheets

Endpoint	Raw Data Location	Dataset Location
Particle size: experiment 1	• Experiment 1:Particle size data – Google Sheets	• Particle size analyses – Google Sheets
Particle size: experiment 2	• Experiment 2: Particle size data – Google Sheets	• Particle size analyses – Google Sheets
Water quality: experiment 1	• Experiment 1: water quality – Google Drive	• Experiment 1: water quality – Google Sheets
Water quality: experiment 2	• Experiment 2: water quality – Google Drive	• Experiment 2: water quality – Google Sheets
Maximum quantum yield (Fv/Fm): experiment 1	• Experiment 1: Fv/Fm – Google Drive	• Experiment 1: Fv/Fm – Google Sheets

Endpoint	Raw Data Location	Dataset Location
Maximum quantum yield (Fv/Fm): experiment 2	• Experiment 2: Fv/Fm – Google Drive	• Experiment 2: Fv/Fm – Google Sheets
Algal symbiont density: experiment 1	• Experiment 1: algal symbiont density – Google Drive	• Experiment 1: algal symbiont density – Google Sheets
Algal symbiont density: experiment 2	• Experiment 2: algal symbiont density – Google Drive	• Experiment 2: algal symbiont density – Google Sheets
Coral buoyant weight: experiment 1	• Experiment 1: buoyant weight – Google Drive (From which dry weights were calculated)	• Experiment 1: buoyant weight – Google Sheets
Coral buoyant weight: experiment 2	• Experiment 2: buoyant weight – Google Drive (From which dry weights were calculated)	• Experiment 2: buoyant weight – Google Sheets
Coral growth (dry weight): experiment 1	• Experiment 1: buoyant weight – Google Drive (From which dry weights were calculated)	• Experiment 1: calculated dry weight – Google Sheets
Coral growth (dry weight): experiment 2	• Experiment 2: buoyant weight – Google Drive (From which dry weights were calculated)	• Experiment 2: calculated dry weight – Google Sheets
Tissue regeneration: experiment 1	• Experiment 1: tissue regeneration – Google Drive	• Experiment 1: tissue regeneration – Google Sheets
Tissue regeneration: experiment 2	• Experiment 2: tissue regeneration – Google Sheets	• Experiment 2: tissue regeneration – Google Sheets
Total lipids/Total proteins: experiment 1	• Experiment 1: total lipids/proteins – Google Drive	• Experiment 1: total lipids/proteins – Google Sheets
Total lipids/Total proteins and TG: experiment 2	• Experiment 2: total lipids/proteins and TG – Google Drive	• Experiment 2: total lipids/proteins and TG – Google Sheets

6.3. Appendix C. ImageJ Macro Code for Lesion Regeneration Assay

```
// Lesion Regeneration Rate
// Chad McCormick 29 August 2009

// global variables
var instance = 0;
var truncPath= "";
var ID = "";
var excelTitle="[Lesion_Data.xls]";

macro "Unused Tool-1 - " {}

macro "Open File and Outline Lesion Action Tool. . . - C059T3e16O"{

// Set Instance to zero if accidentally close xls file BACKUP
list=getList("window.titles");
newDataSet=1;
for(i=0;i<list.length;i++){
        if (list[i]=="Lesion_Data.xls"){
                newDataSet=0;
        }
}

if (newDataSet!=0){
instance=0;
}

// Make table to store measurements
if(instance==0){
run("Table...", "name=Lesion_Data.xls");
print(excelTitle, "\\Headings:n\tImage Title\tPixels/mm\tArea (mm^2)\tPerim (mm)");
}
instance++;

// Set measurements
run("Set Measurements...", "area perimeter display redirect=None decimal=2");

// Open file
path=File.openDialog("Lesion File to Analyze:");
open(path);
truncPath=nameLabel(path);
ID=getTitle();

//1. User starts with two boxes.  Moves one over lesion, one over ruler. (1.jpg)

run("Original Scale"); // No zoom yet
roiManager("Reset"); // No Rois yet
setTool(0); // Use box tool to adjust size and/or location of boxes

// Lesion box
makeRectangle(1592, 836, 524, 524);
roiManager("Add");
roiManager("Select",0);
```

```
lTitle="Select Region Around Lesion";
lMsg="Select region encompassing lesion for zoom.\nThen click \"OK\"";
waitForUser(lTitle,lMsg);
roiManager("Update");
roiManager("Rename", "Lesion Box");

// Ruler box
rTitle="Select Region Around Ruler";
rMsg="Select region encompassing ruler for zoom.\nThen click \"OK\"";
makeRectangle(1304, 1580, 1108, 504);
roiManager("Add");
roiManager("Select",1);
waitForUser(rTitle,rMsg);
roiManager("Update");
roiManager("Rename", "Ruler Box");


/*2. Zoom in on lesion and outline lesion manually with freehand selection.
This may be easier if you purchased a $20 USB graphics tablet, but teaching
this you can just use a mouse.  The user can modify his/her selection
accordingly as I show a relatively poor outline. (2.jpg)
*/

roiManager("Select", 0);
run("To Selection");
setTool(3);
leTitle="Trace Edges of Lesion";
leMsg="Follow edges of lesion with mouse.\nThen click \"OK\"";
run("Select None"); // Remove box
roiManager("Deselect"); // No rois selected
waitForUser(leTitle,leMsg);
getSelectionCoordinates(x, y);
run("Select None");
makeSelection("polygon", x, y);
roiManager("Add");

roiManager("Select", 2);
moTitle="Modify outline?";
moMsg="Use mouse to move any incorrect verticies.\nThen click \"OK\"";
waitForUser(moTitle,moMsg);
roiManager("Update");
roiManager("Rename","Lesion");

// 3. Zoom in on ruler and draw line on the edge of the ruler a certain size
//(I prefer 5 cm to average out some of the error in tracing this distance). (3.jpg)

setTool(4);
roiManager("Select", 1);
run("To Selection");
run("Select None");
roiManager("Deselect");
ruTitle="Trace 3 mm";
ruMsg="Trace 3 mm on edge of ruler.\nThen click \"OK\"";
waitForUser(ruTitle,ruMsg);
roiManager("Add");
roiManager("Select",3);
```

```
roiManager("Rename", "3 mm");
getLine(x1, y1, x2, y2,width);
dx = x2-x1; dy = y2-y1;
length = sqrt((dx*dx)+(dy*dy));
run("Set Scale...", "distance="+length+" known=3 pixel=1 unit=mm");
units=length/3;


// 4. Save region information with image name.

roiManager("Deselect");
roiManager("Save",truncPath+".zip");

// 5. Start excel file with name and area per lesion. (4.jpg area in mm2).
roiManager("Select",2);
getStatistics(area,perimeter,mean,min,max,std);
print(excelTitle, instance+"\t"+ID+"\t"+units+"\t"+area+"\t"+perimeter+"\n");
run("Select None");
roiManager("Deselect");

// Close Windows
selectWindow(ID);
run("Close");
roiManager("Reset");
}

// 6. Save excel file when done series of images.

macro "Save Excel Data Action Tool. . . - C059T3e16S"{
list=getList("window.titles");
for(i=0;i<list.length;i++){
	if (list[i]=="Lesion_Data.xls"){
		selectWindow("Lesion_Data.xls");
		saveAs("Text");
		selectWindow("Lesion_Data.xls");
		run("Close");
	}

	else if (list[i]=="ROI Manager"){
		selectWindow("ROI Manager");
		run("Close");
	}
}

instance=0;

}

// FUNCTIONS //
function nameLabel(name){
	namePrefix=split(name,".");
	labelName=namePrefix[0];
	return labelName;
}
```

6.4. Appendix D. Protocol Directory with Links to Google Drive

Protocol Title	Protocol Link to Google Drive Location
• Appx. 6.4.D1 Experimental Protocol: Long-term Turbidity Dose-Response	• Turbidity dose-response experiment protocol – Google Drive
• Appx. 6.4.D2 Experimental Protocol: Long-term Turbidity and Temperature Dual-Stressor Exposure	• Dual stressor experiment protocol – Google Drive
• Appx. 6.4.D3 Cleaning Protocol for Materials used in Turbidity Experiments	• Turbidity equipment cleaning protocol – Google Drive
• Appx. 6.4.D4 Particle Size Analysis Protocol	• Particle size analysis protocol and technical procedure – Google Drive
• Appx. 6.4.D5 Measuring Chlorophyll *a* Fluorescence of Coral Symbionts using the Imaging Maxi Pulse Amplitude Modulated (PAM) Fluorometer	• PAM fluorometry protocol – Google Drive
• Appx. 6.4.D6 Dinoflagellate Symbiont Density Measurements from Histological Sections	• Dinoflagellate symbiont density protocol – Google Drive
• Appx. 6.4.D7 Measuring Calcium Carbonate Deposition as a Proxy for Coral Growth	• Buoyant weight protocol – Google Drive
• Appx. 6.4.D8 Determining Coral Tissue Regeneration following Wounding	• Tissue regeneration assay protocol – Google Drive
• Appx. 6.4.D9 SIMPLEX Protocol for Protein and Lipid Extractions	• Total lipids and total soluble proteins protocol – Google Drive
• Appx. 6.4.D10 Determination of Triglyceride (TG) Concentration from Coral Tissue	• Triglyceride assay protocol – Google Drive